REPORT SAMSO-TR-77-200

Characteristics of 5- to 35- Turn Uniform Helical Antennas

Electronics Research Laboratory
The Ivan A. Getting Laboratories
The Aerospace Corporation
El Segundo, Calif. 90245

1 June 1977

Final Report

Prepared for
SPACE AND MISSILE SYSTEMS ORGANIZATION
AIR FORCE SYSTEMS COMMAND
Los Angeles Air Force Station
P.O. Box 92960, Worldway Postal Center
Los Angeles, Calif. 90009

This report was submitted by The Aerospace Corporation, El Segundo, CA 90245, under Contract F04701-76-C-0077 with the Space and Missile Systems Organization, Deputy for Advanced Space Programs, P.O. Box 92960, Worldway Postal Center, Los Angeles, CA 90009. It was reviewed and approved for The Aerospace Corporation by A. H. Silver, Director, Electronics Research Laboratory, and E. T. Bobak, Systems Engineering Operations.

This report has been reviewed by the Information Office (OI) and is releasable to the National Technical Information Service (NTIS). At NTIS, it will be available to the general public, including foreign nations.

This technical report has been reviewed and is approved for publication. Publication of this report does not constitute Air Force approval of the report's findings or conclusions. It is published only for the exchange and stimulation of ideas.

Dara Batki
Dara Batki, Lt, USAF
Project Officer

Robert W. Lindemuth
Robert W. Lindemuth, Lt. Col, USAF

FOR THE COMMANDER

Leonard E. Baltzell, Col, USAF
Assistant Deputy for Advanced
Space Programs

UNCLASSIFIED

SECURITY CLASSIFICATION OF THIS PAGE (When Data Entered)

(19) REPORT DOCUMENTATION PAGE	READ INSTRUCTIONS BEFORE COMPLETING FORM
1. REPORT NUMBER (18) SAMSO-TR-77-200	2. GOVT ACCESSION NO.
3. RECIPIENT'S CATALOG NUMBER	
4. TITLE (and Subtitle) (6) CHARACTERISTICS OF 5- TO 35- TURN UNIFORM HELICAL ANTENNAS	5. TYPE OF REPORT & PERIOD COVERED (9) Final rept.
6. PERFORMING ORG. REPORT NUMBER (14) TR-0078(3724-01)-2	
7. AUTHOR(s) (10) H. E. King and J. L. Wong	8. CONTRACT OR GRANT NUMBER(s) (15) F04701-76-C-0078
9. PERFORMING ORGANIZATION NAME AND ADDRESS The Aerospace Corporation El Segundo, Calif. 90245	10. PROGRAM ELEMENT, PROJECT, TASK AREA & WORK UNIT NUMBERS (12) 53 p.
11. CONTROLLING OFFICE NAME AND ADDRESS	12. REPORT DATE (11) 1 Jun 77
	13. NUMBER OF PAGES 50
14. MONITORING AGENCY NAME & ADDRESS (if different from Controlling Office) Space and Missile Systems Organization Air Force Systems Command Los Angeles Air Force Station, P.O. Box 92960 Worldway Postal Center Los Angeles, California 90009	15. SECURITY CLASS. (of this report) Unclassified
	15a. DECLASSIFICATION/DOWNGRADING SCHEDULE

16. DISTRIBUTION STATEMENT (of this Report)

Approved for public release; distribution unlimited

17. DISTRIBUTION STATEMENT (of the abstract entered in Block 20, if different from Report)

18. SUPPLEMENTARY NOTES

19. KEY WORDS (Continue on reverse side if necessary and identify by block number)

Helical Antennas
Cavity-Backed Helices
Fixed Length Helices
Variable Length Helices
Constant Pitch Helix
lamda

20. ABSTRACT (Continue on reverse side if necessary and identify by block number)

The measured VSWR, gain, pattern and axial ratio characteristics of a uniformly wound helical antenna are presented. Experimental parametric studies were made of 1) fixed length helices with variable diameter and pitch angle (8.6 to 10 turns), and 2) variable length helices with constant diameter and pitch angle (5 to 35 turns). Simplified design relations are given for the antenna gain and half-power beamwidth (HPBW) as a function of axial length L/λ and circumference C/λ for helices consisting of approximately 10 turns.

DD FORM (FACSIMILE) 1473

409 944

UNCLASSIFIED

SECURITY CLASSIFICATION OF THIS PAGE (When Data Entered)

19. KEY WORDS (Continued)

lamda

20. ABSTRACT (Continued)

Parametric curves are presented to show the gain and HPBW of a constant pitch helix as a function of L/λ and C/λ. An empirical expression is derived for the antenna gain as a function of frequency and the helix design parameters. In addition, the bandwidth characteristics are analyzed.

PREFACE

The authors wish to thank the FleetSatCom Program Office, H. F. Meyer (Director) and P. J. Parszik for their interest and support of this antenna development. Thanks also go to G. G. Berry, L. U. Brown, H. B. Dyson, B. A. Jacobs, O. L. Reid and J. T. Shaffer for constructing and testing of the various antennas.

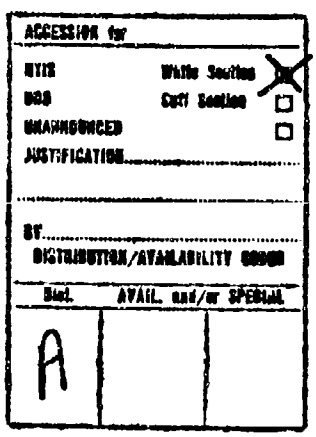

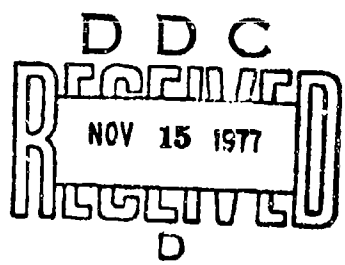

CONTENTS

LIST OF FIGURES

FIGURES (continued)

FIGURES (concluded)

I. INTRODUCTION

The basic concepts of an axial-or beam-mode helical antenna were established by Kraus [Refs. 1,2] in 1947 and summarized by Harris [Ref. 3]. More recently, Maclean and Kouyoumjian [Ref. 4], Maclean and Farvis [Ref. 5] and Maclean [Ref. 6] investigated the bandwidth characteristics and the low- and high-frequency limits for a class of helical antennas. The helical beam antenna is a very simple structure possessing a number of interesting properties including wideband impedance characteristics and circularly-polarized radiation. It requires a simple feed network, and it is simple to build with relatively predictable results. Some measurements have been made to determine the characteristics of helical antennas [Refs. 2, 4, 7]; however, wide bandwidth gain characteristics are generally not available in the open literature. The purpose of the present study was to evaluate the pattern and gain characteristics of helical antennas, 1 to 9 wavelengths long, in the UHF frequency range from about 650 to 1100 MHz. A circular cavity was used to back the helix, rather than a conventional ground plane.

Gain and pattern data were obtained on fixed-length (30.8 in.) helices consisting of 8 to 10 turns with a variable diameter and pitch angle. Also, with a fixed diameter and pitch, the gain and pattern characteristics were measured for helices consisting of 5 to 35 turns. The measured gain and half-power beamwidth are presented parametrically with respect to C/λ and L/λ, where λ is the free space wavelength, C is the circumference and L is the length of the helix. Empirical relations are derived which express the antenna gain as a function of wavelength and the helix design parameters (diameter, pitch angle, and number of turns). In addition, the gain-beamwidth product and the beamwidth and gain factors are examined. For this study all the helices were wound with a uniform diameter. It is shown in a separate study [Refs. 8 and 9] that by tapering the last two turns of the helix, the VSWR, pattern and axial ratio characteristics can be improved significantly over those of a completely uniform helix.

II. GENERAL DISCUSSION

A. DESCRIPTION OF ANTENNAS

The antenna was made by winding 3/16-in. diameter copper tubing around a styrofoam cylindrical form. The helix diameter is defined as the center-to-center distance of the copper wire. A 1.125-in. diameter aluminum tubing was inserted coaxially into the foam to provide mechanical rigidity. A circular cavity was used to reduce the back radiation and enhance the forward gain. A cavity diameter of 10.3 in. was found to be approximately optimum for a 10-turn helix based on measurements. The overall length of the helix = $NS + L_F$, where N = number of turns, S = separation between turns, and L_F = length of the feed point ~ 0.8 in. (L_F is the distance from the cavity bottom to the start of the first turn of the helix). Figure 1 shows the mechanical arrangement.

B. MEASUREMENTS

VSWR, gain, radiation patterns, and axial ratio measurements were made on the various helices described in this report. The VSWR characteristics of the various helices are similar over the frequency range of interest; thus, only representative curves will be shown. The gain, radiation patterns or halfpower beamwidths (HPBW), and axial ratios will be shown for each of the helix antennas.

A microstrip transformer, constructed from a teflon-fiberglass printed circuit board and placed on the bottom of the cavity (inside), was used to match the helix impedance ($\sim 140\Omega$) to a 50Ω coaxial input. The 4.7-in. length transformer consisted of a linear taper of the microstrip width. The impedance characteristics of a 5-turn helix with and without the impedance matching transformer are shown in Fig. 2. Figure 3 depicts the VSWR response measured at the input of the matching transformer of a 5-, 12-, and 35-turn uniform helix.

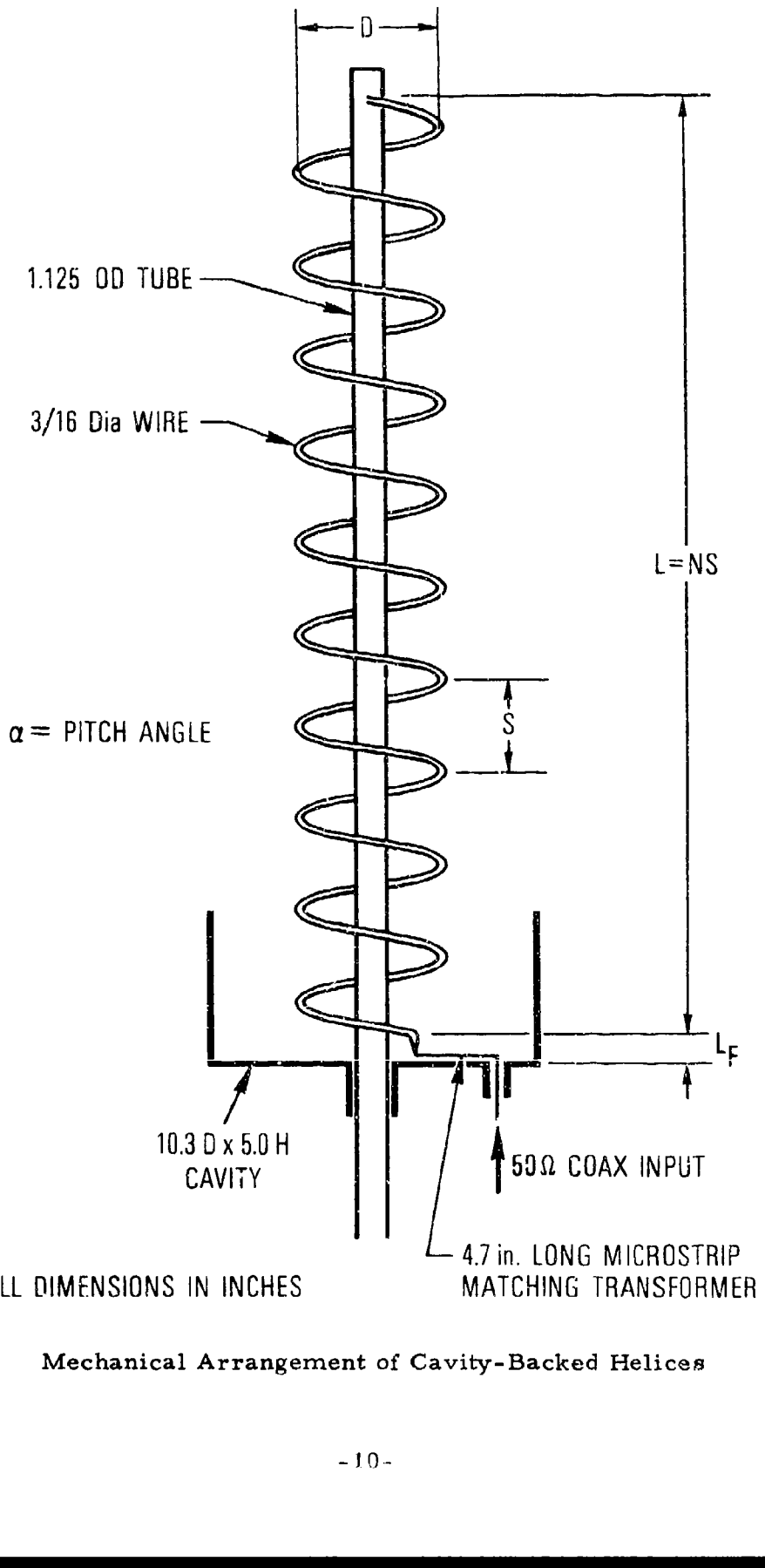

Fig. 1 Mechanical Arrangement of Cavity-Backed Helices

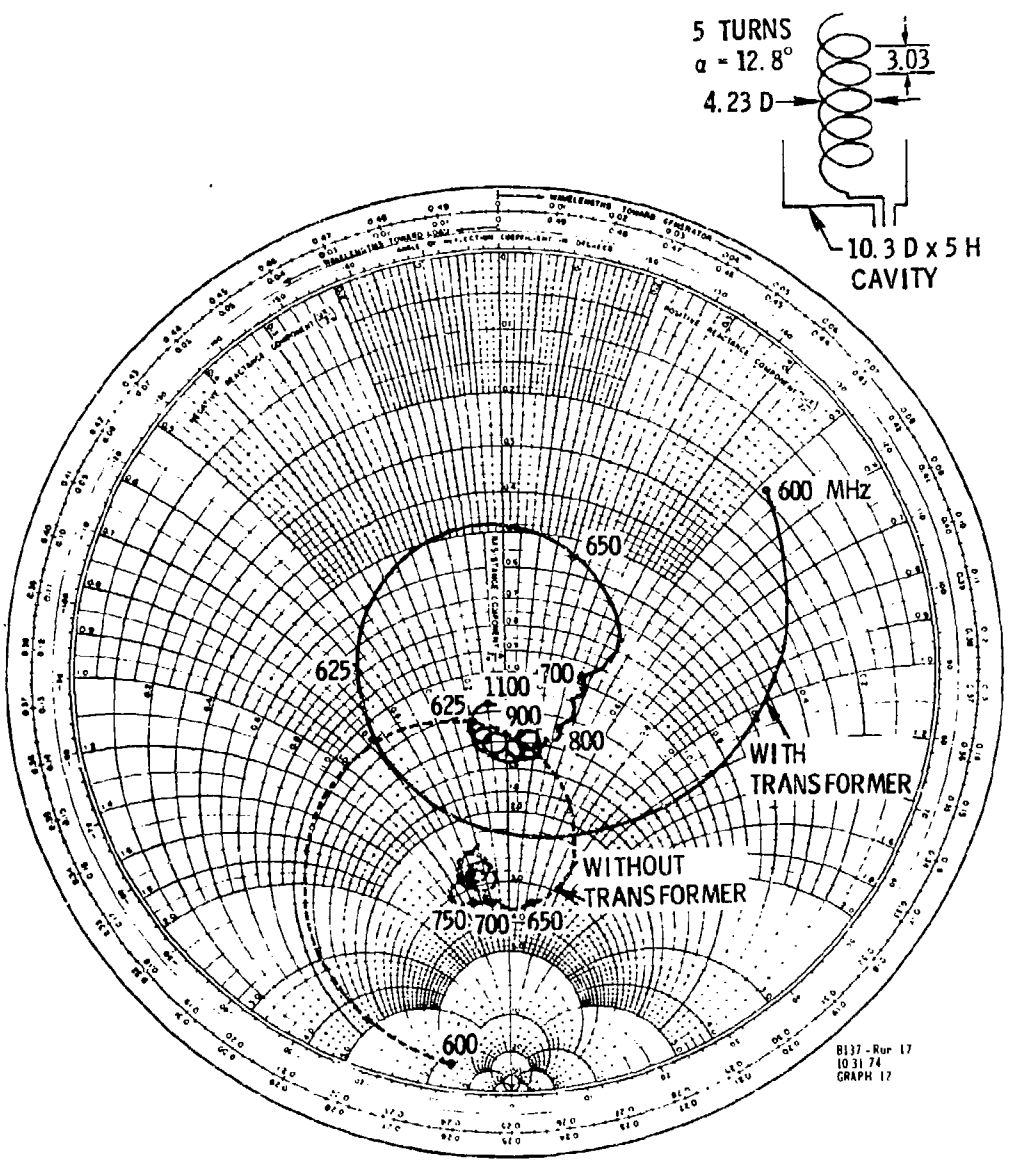

Fig. 2 Impedance Characteristics of a 5-Turn Helix With and Without an Impedance-Matching Transformer

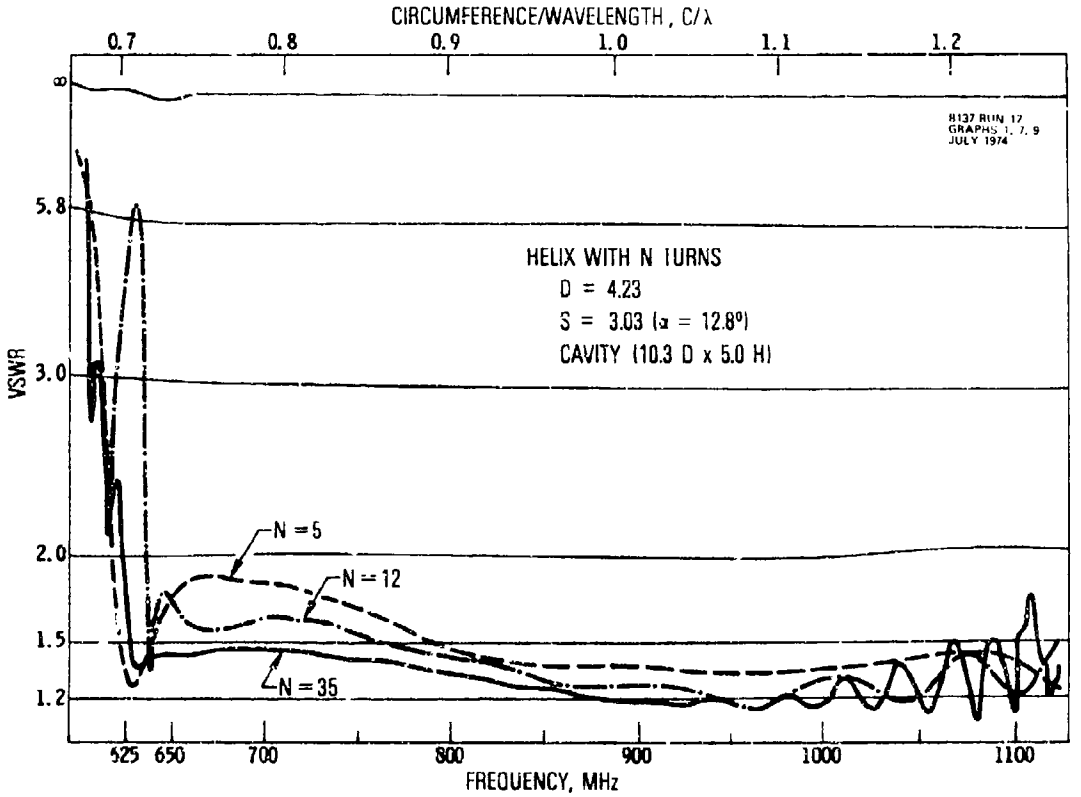

Fig. 3 VSWR Responses of 5, 12, and 35 Turn Helices With Impedance-Matching Transformers

The gain, pattern and axial ratio measurements were made on an antenna range with a spacing between the helix and source antenna of 30 to 60 ft and with the antennas approximately 16 ft above the ground. Repeated measurements at different range distances were made and averaged to minimize the effects of multipath errors. To minimize the parallax in the pattern measurements, the helix was rotated about the helix phase center which was estimated to be approximately 1/4 the length of the helix from the feed point [Ref. 10].

Gain measurements were accomplished by the "substitution" method. The phase center of the helix was used as the spatial reference plane; i.e., the standard gain antenna was placed at the spatial reference plane. A linearly-polarized reference-gain horn (Nurad, Inc., Model 7 RH) antenna was calibrated using the conventional "two-antenna" method. Using a linearly-polarized source antenna, the gain of the helix was obtained by comparing the total received power in two orthogonal polarizations of the helix and the power received by the reference-gain antenna. The helix antenna gain with respect to a circularly-polarized illuminating source was computed by measuring the axial ratio and correcting for the polarization mismatch loss with respect to circular polarization. Repeated measurements were made to improve the accuracy. Thus, the gain data presented herein represents a "smooth-fit" curve to the data points.

The axial ratios and HPBWs represent average values as determined from two or more repeated pattern measurements in two principal planes of the helix and/or at different range distances between the helix and the source. In addition, some of the data were obtained by repeated measurements of a second helix constructed with the same mechanical dimensions. Generally, the axial ratio variations were less than a few-tenths of a dB and the HPBWs are within $\pm 1^{\circ}$ in the two principal planes ($\phi = 0^{\circ}$ and 90°). Beam symmetry were reasonably good for all the helices; thus, patterns will be shown for only one principal plane.

III. GAIN AND PATTERN CHARACTERISTICS

A. FIXED LENGTH HELIX

Parametric evaluations were made to establish the gain and pattern characteristics of a fixed length helix with 1) a variable pitch angle and a constant diameter, and 2) a variable diameter and a fixed number of turns (N = 10).

The gain vs frequency characteristics of a 30.8-in. long and 4.3-in. diameter helix are shown in Fig. 4, for three helix pitch angles (α = 12.5°, 13.5° and 14.5°). Note the 30.8-in. length dimension includes 0.8-in. for the feed strap. For these helices, the gain peaks approximately at $C/\lambda \sim 1.13$ to 1.14. The helix with a smaller pitch angle (more turns per unit length) yields a higher peak gain and a lower cutoff frequency. To illustrate the frequency dependence, the dotted line shows a gain-frequency slope proportional to f^3, where f = frequency. Thus, it appears that the gain-frequency characteristics of Fig. 4 with N = 8.6 to 10 turns are in general agreement with Kraus [Refs. 1,2] for $C/\lambda < 1.1$. However, as will be shown later, experimental data indicate that the gain-slope depends on the antenna length and is approximately proportional to $f^{\sqrt{N}}$.

Figure 5 shows the gain vs frequency characteristics of a 30.8-in. long helix (N ≈ 10 turns) with variable diameter and pitch angle. The peak gains are approximately the same and occur at $C/\lambda \sim 1.135$ on the average. A slightly higher peak gain is observed for the larger diameter (D = 4.69 in.) helix with a smaller pitch angle, but the bandwidth is narrower. The gain curves also show little change at the low frequency end for the 4.13-in. and 4.23-in. diameter helices. However, a higher upper-frequency limit, and thus wider bandwidth, is attained for helices with a larger pitch angle, which agrees with theory.

Based on the gain data of Figs. 4 and 5, the peak gain may be empirically expressed as

$$G_p = 8.3 \left(\frac{\pi D}{\lambda_p}\right)^{\sqrt{N+2}-1} \left(\frac{NS}{\lambda_p}\right)^{0.8} \left[\frac{\tan 12.5^\circ}{\tan \alpha}\right]^{\sqrt{N}/2} \qquad (1)$$

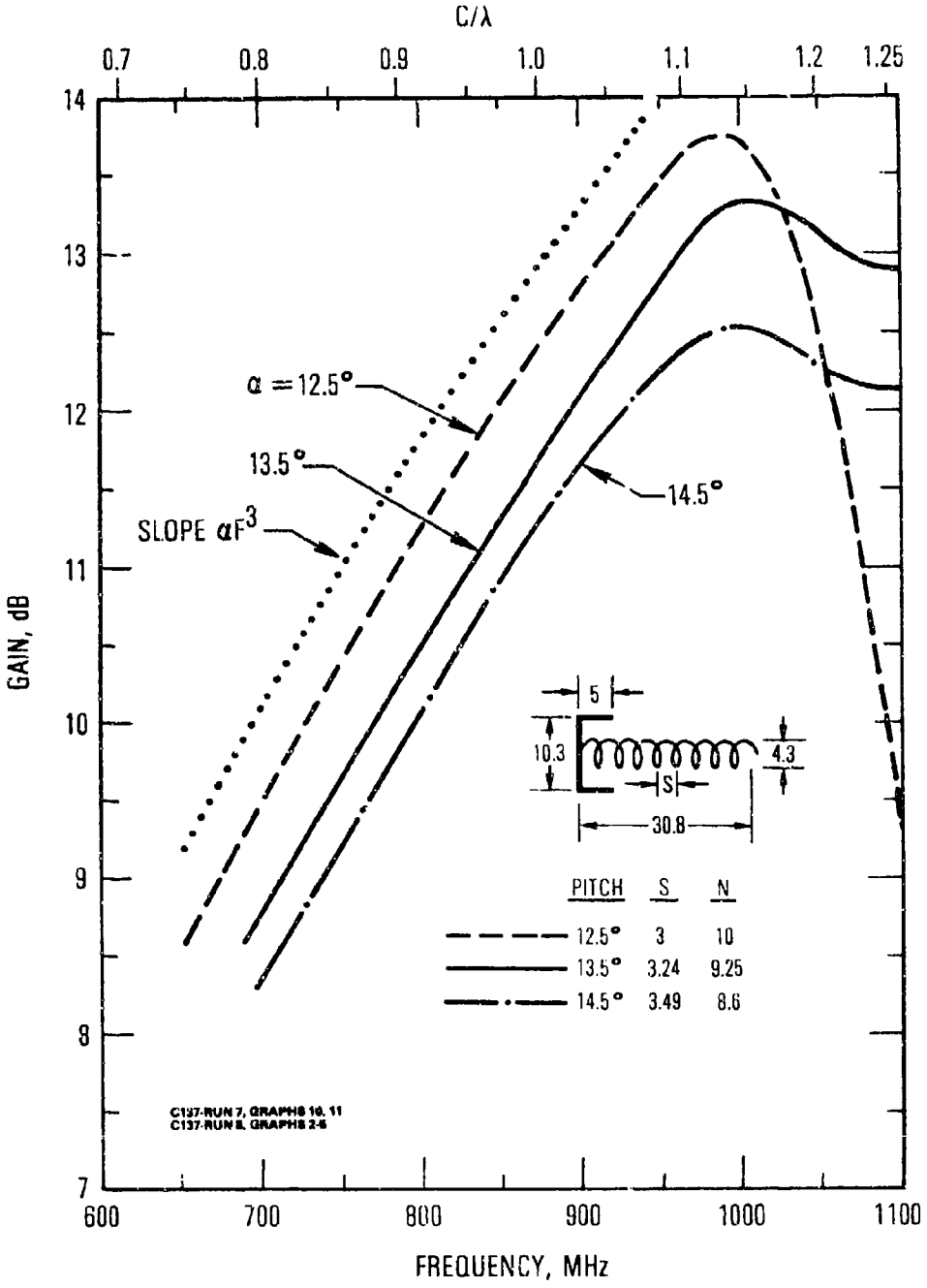

Fig. 4 Helical Antenna Gain of a 30.8-in. Length and 4.3-in. Diameter Helix for Pitch Angles = 12.5°, 13.5° and 14.5°.

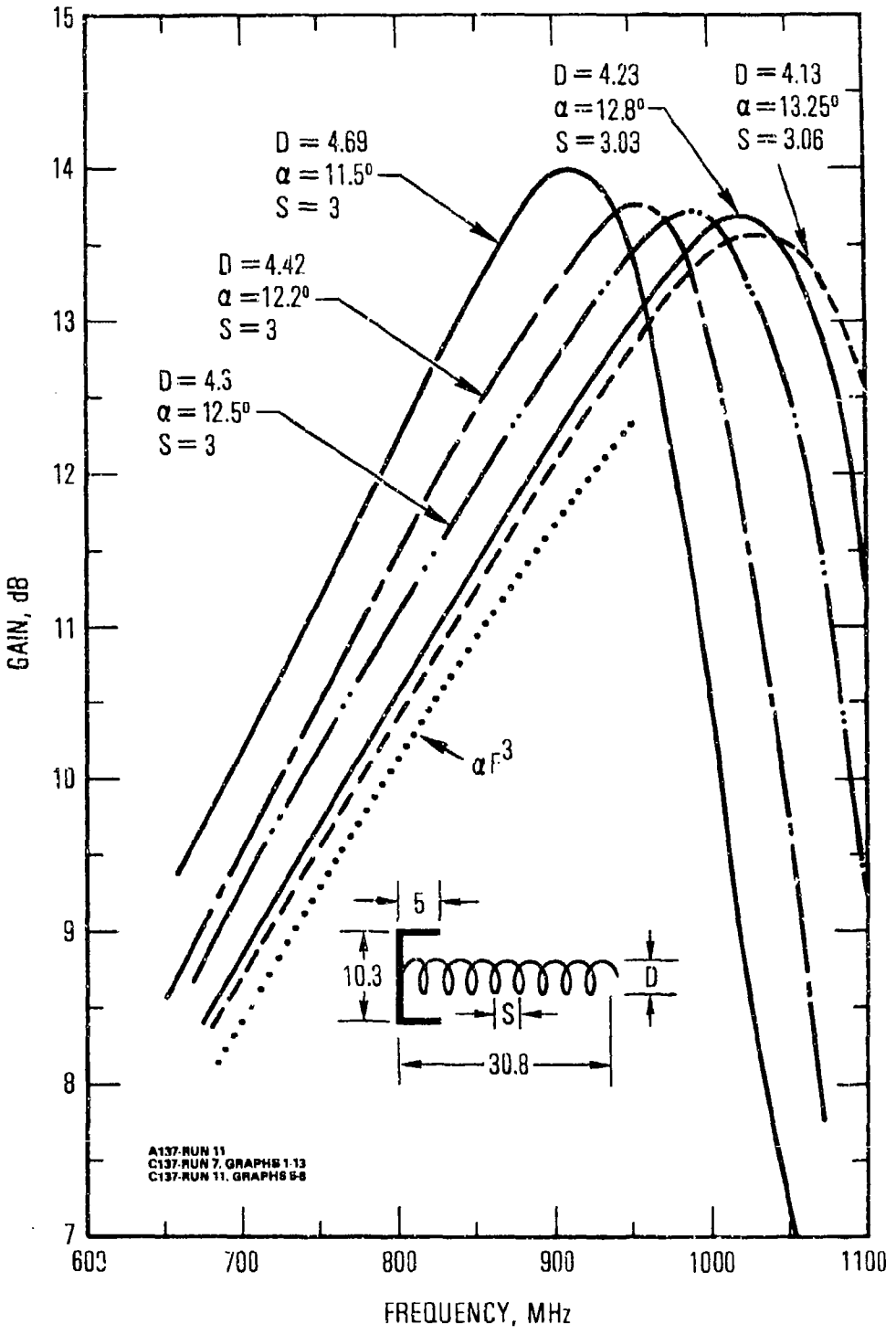

Fig. 5 Gain of Fixed-Length (30.8 in.) Helical Antenna for Various Diameters

where λ_p is the wavelength at peak gain and α is the pitch angle. Note that $S = \pi D \tan \alpha$ and NS = constant for a fixed length helix. The computed values are within $\pm$ 0.1 dB of the measured data as depicted in Fig. 6. The data points indicated by o were obtained by varying the diameter and pitch angle while keeping the length constant with $N \approx 10$ turns, and those indicated by Δ were obtained by varying the pitch angle while keeping the length and diameter constant ($N \approx 8.6$ to 10 turns). The diameters of the various experimental helices are shown on the top of the figure. It is also interesting to note that, for these fixed-length helices, the peak gains occur at nearly the same circumference $\pi D/\lambda \sim 1.135$ as shown in Fig. 6.

The radiation patterns for a 30.8-in. long, 10-turn helix with D = 4.42 in. and $\alpha = 12.2^\circ$ are shown in Fig. 7. The measured patterns at 1030 MHz ($C/\lambda = 1.21$) show that the first sidelobes begin to merge with the main lobe, which effectively increases the HPBW with a corresponding reduction in gain. At 1067 MHz ($C/\lambda = 1.25$) the main lobe has encompassed the first sidelobes with a marked drop in gain as can be seen from Fig. 5. To illustrate the pattern symmetry, two principal plane cuts are shown for 725, 850 and 1000 MHz. Rather than presenting all of the measured patterns, the HPBWs are plotted in Fig. 8 for the 4.3-in. diameter helix with variable pitch angles (11.5°, 12.5° and 13.5°), and in Fig. 9 for the 30.8-in. length helix with variable diameters (4.13 to 4.69 inches). A slope proportional to $F^{-3/2}$ is shown for reference in Figs. 8 and 9.

To provide parametric design equations for helices, Kraus [Ref. 2] has suggested the following relations for the gain and HPBW as a function of C/λ and L/λ for constant pitch helices with $12^\circ < \alpha < 15^\circ$, $3/4 < C/\lambda < 4/3$, and $N > 3$:

$$G = K_G (C/\lambda)^2 \ (L/\lambda) \tag{2}$$

$$\text{HPBW} = \frac{K_B}{\left(\frac{C}{\lambda}\right)\sqrt{L/\lambda}} \tag{3}$$

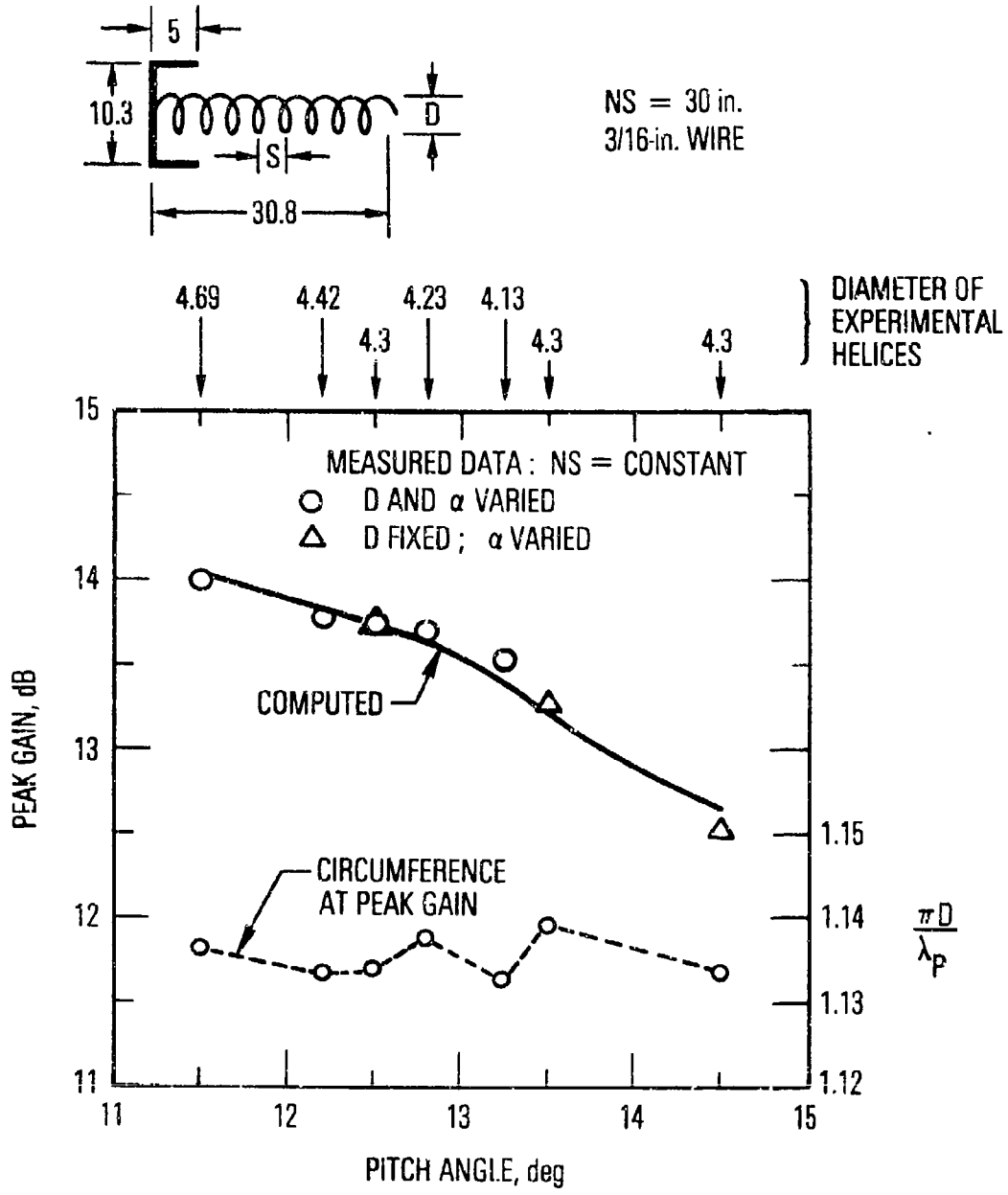

Fig. 6 Peak Antenna Gain Characteristics of a Helix with a Fixed Length and for Various Diameters and Pitch Angles.

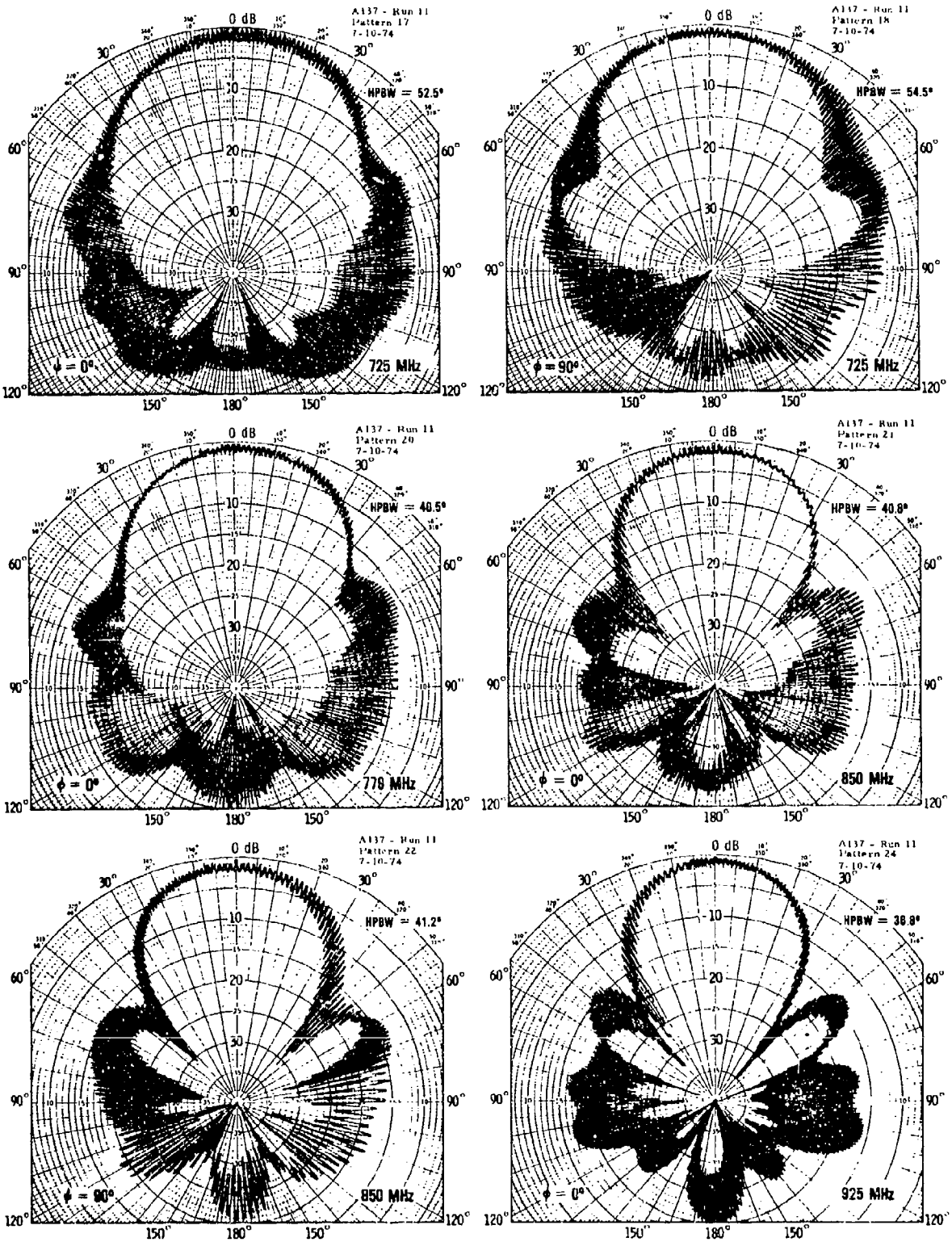

Fig. 7 Radiation Patterns for a 10-turn Helix, 30.8-in. Long x 4.42- in. Diameter with a 12.2° Pitch Angle (S = 3 in.).

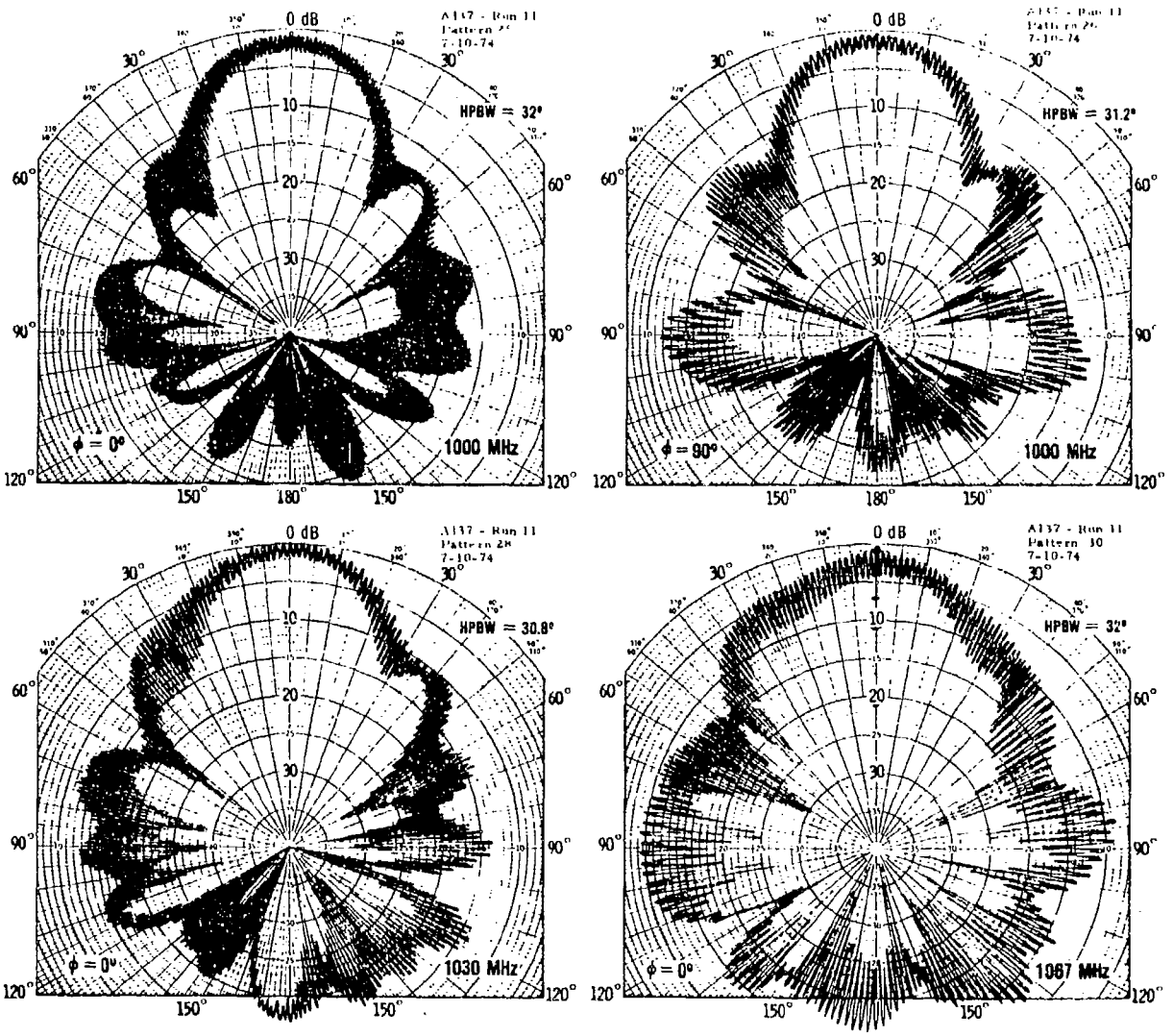

Fig. 7 (concluded)

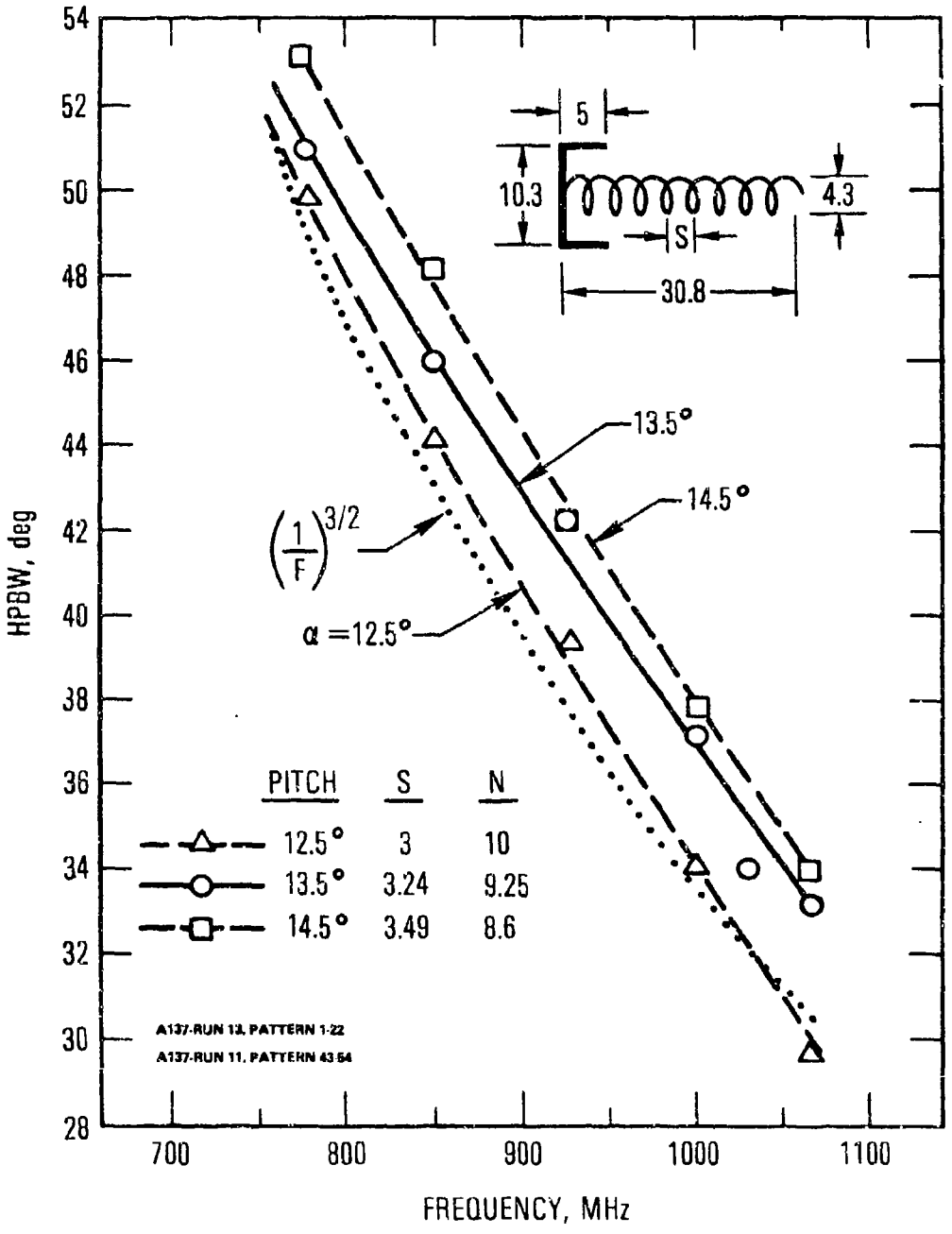

Fig. 8 Halfpower Beamwidths of a 30.8-in. Length and 4.3-in. Diameter Helix for Pitch Angles = 12.5°, 13.5° and 14.5°.

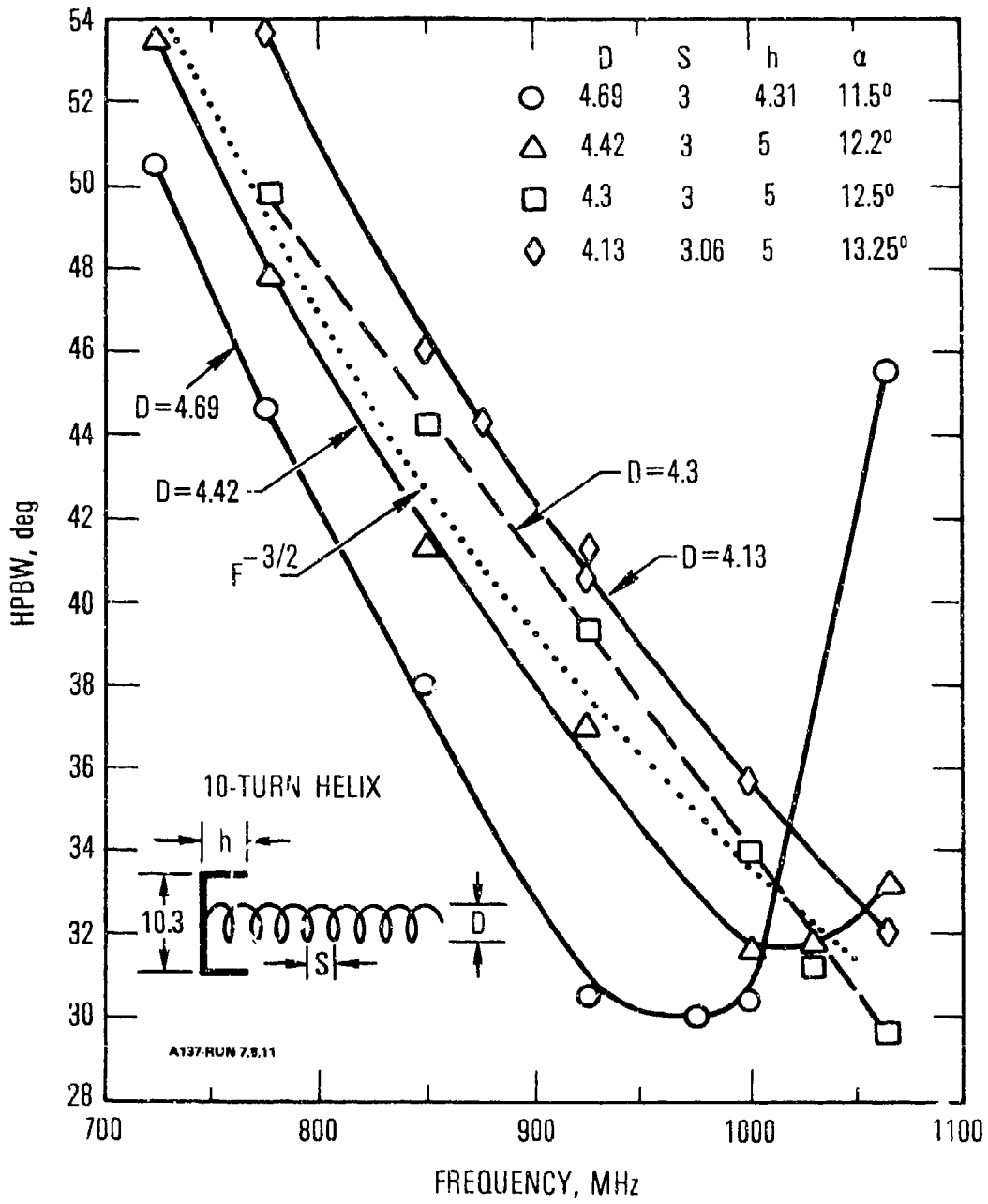

Fig. 9 **Halfpower Beamwidths of a 10-turn Helix 30.8-in. Long, for Diameters = 4.13 to 4.69 inches.**

where K_G is the gain factor, K_B is the HPBW factor, $C = \pi D$ is the circumference and $L = NS$ is the axial length. The measured gain and HPBW factors for the 30.8-in. length (NS = 30 in.) and 4.3-in. diameter helices are shown in Figs. 10 and 11, respectively. It can be seen that a higher gain is obtained with a smaller pitch angle for a given length (note there are more turns per unit length). Also, it is interesting to note that, for a given pitch angle, the gain factor remains essentially constant for $0.8 < C/\lambda < 1.09$. Within this range of circumference, the gain factor varies from about 5.8 for $\alpha = 14.5^{\circ}$ to about 7.6 for $\alpha = 12.5^{\circ}$. As will be shown later, the gain and HPBW factors [Eqs. (2) and (3)] are relatively constant only for helices with approximately 10 turns.

Based on a large number of pattern measurement, Kraus has quasi-empirically established $K_B = 52$ for the HPBW. Also, he derived $K_G = 15$ for the directive gain (lossless antenna) based on the approximation $G = 41,250/\theta^2$, where θ is the HPBW in degrees. A $G\theta^2$ product $< 41,250$ is generally expected for most practical antennas [Ref. 11] because of minor lobe radiation and beam shape variations.

The measured HPBW factors of Fig. 11 vary from about 61 to 70 (compared with Kraus' empirical value of 52) for $0.8 < C/\lambda < 1.2$, and the gain factors, varying from about 4.2 to 7.7 over the same C/λ range, are considerably lower than Kraus' estimated value of 15. The wide beamwidth characteristics for the helices considered are believed to be partially attributed to 1) the fact that the amplitude and phase characteristics along the helix probably deviate from those required to satisfy the Hansen-Woodyard increased directivity condition, 2) the effects of the ground plane or cavity which may alter the beam shape and minor lobe characteristics, and 3) construction tolerances.

Another design relation, which is often used, expresses the gain as a function of the HPBW, or

$$G = K/\theta^2 \tag{4}$$

where θ = HPBW and K is referred as the gain-beamwidth product. The

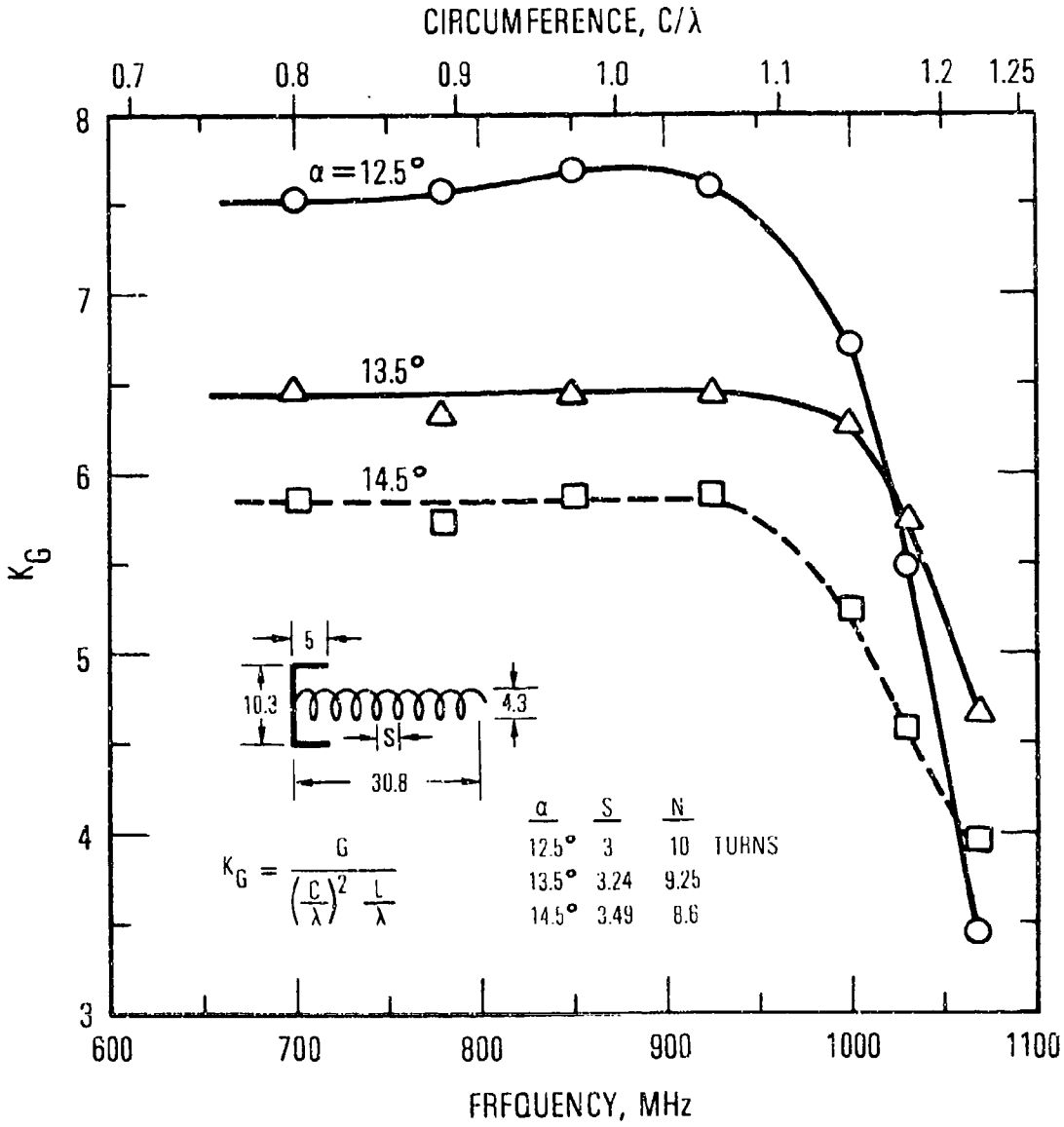

Fig. 10 Gain Factor as a Function of Length and Diameter for Various Pitch Angles Based on the 30.8-in. Length, 4.3-in. Diameter Experimental Helix

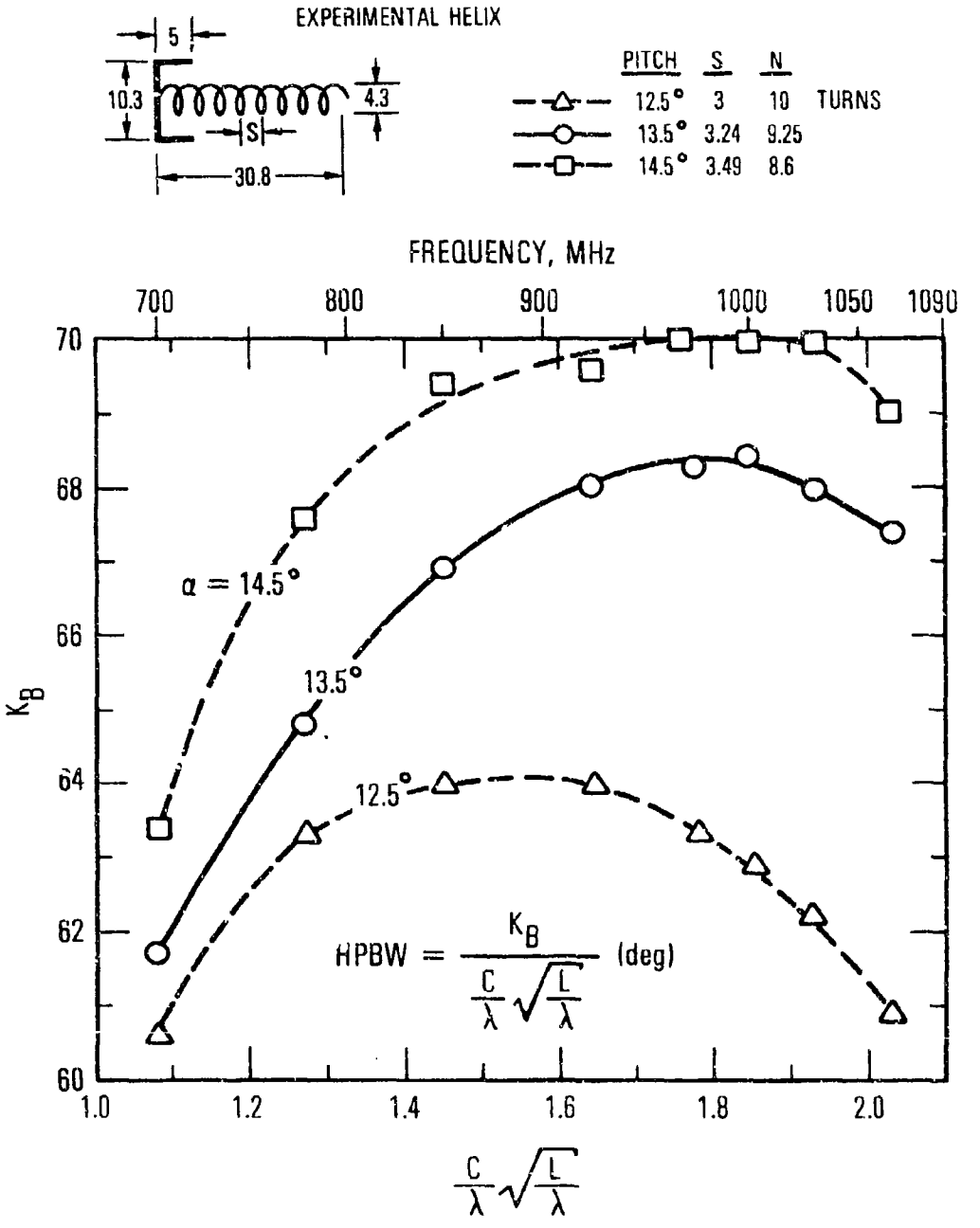

Fig. 11 Beamwidth Factor as a Function of Circumference and Length of Helix for Various Pitch Angles Based on the 30.8-in. Length, 4.3-in. Diameter Experimental Helix

empirical values of the gain-beamwidth product as derived from the curves of Figs. 4 and 8 are shown in Fig. 12. For $0.8 < C/\lambda < 1.16$, the gain-beamwidth product varies from 24,000 to 31,500 as compared with 41,250 when the minor lobes are neglected.

The axial ratio characteristics for a fixed-length helix with a constant diameter and variable pitch angle are shown in Fig. 13, while those for a 10-turn, fixed-length helix and variable diameter are shown in Fig. 14. Generally, the axial ratio is less than 1.5 dB for $0.8 < C/\lambda < 1.2$. It has been shown in a separate study that, by tapering the last 2 turns of the helix, the axial ratio can be improved considerably over the useful frequency range of the helix, particularly at the high end of the band [Ref. 8].

B. VARIABLE LENGTH HELIX

Parametric evaluations were made to establish the gain and pattern characteristics of a constant pitch helix consisting of 5 to 35 turns. The 4.23-in. diameter was selected so that the helix would operate over the UHF test frequencies with a helix circumference ranging from about 0.75λ to 1.25λ. A 12.8° pitch angle was chosen, which corresponds to a spacing S = 3.03 inches. N was selected as 5, 10, 12, 15, 18, 22, 26, 30, and 35 turns.

Gain vs frequency for the various values of N are plotted in Fig. 15. The gain is referred to a circularly polarized illuminating source. The gain curves reveal that the peak gain occurs at $C/\lambda = 1.155$ for N = 5 and decreases to $C/\lambda = 1.07$ for N = 35. For reference, the dotted lines provide an estimate of the gain variations with frequency; e.g., for N = 5 the gain varies approximately as $f^{2.5}$, and for N = 35 the gain follows approximately a f^{6} slope, where f = frequency. Note that the measured gain slope is proportional to f^{3} only when N is approximately 10 turns (see also Figs. 4 and 5).

Figure 16 is a plot of the peak gain vs the number of turns for the 4.23-in. diameter helix. The corresponding values of C/λ_p are also shown

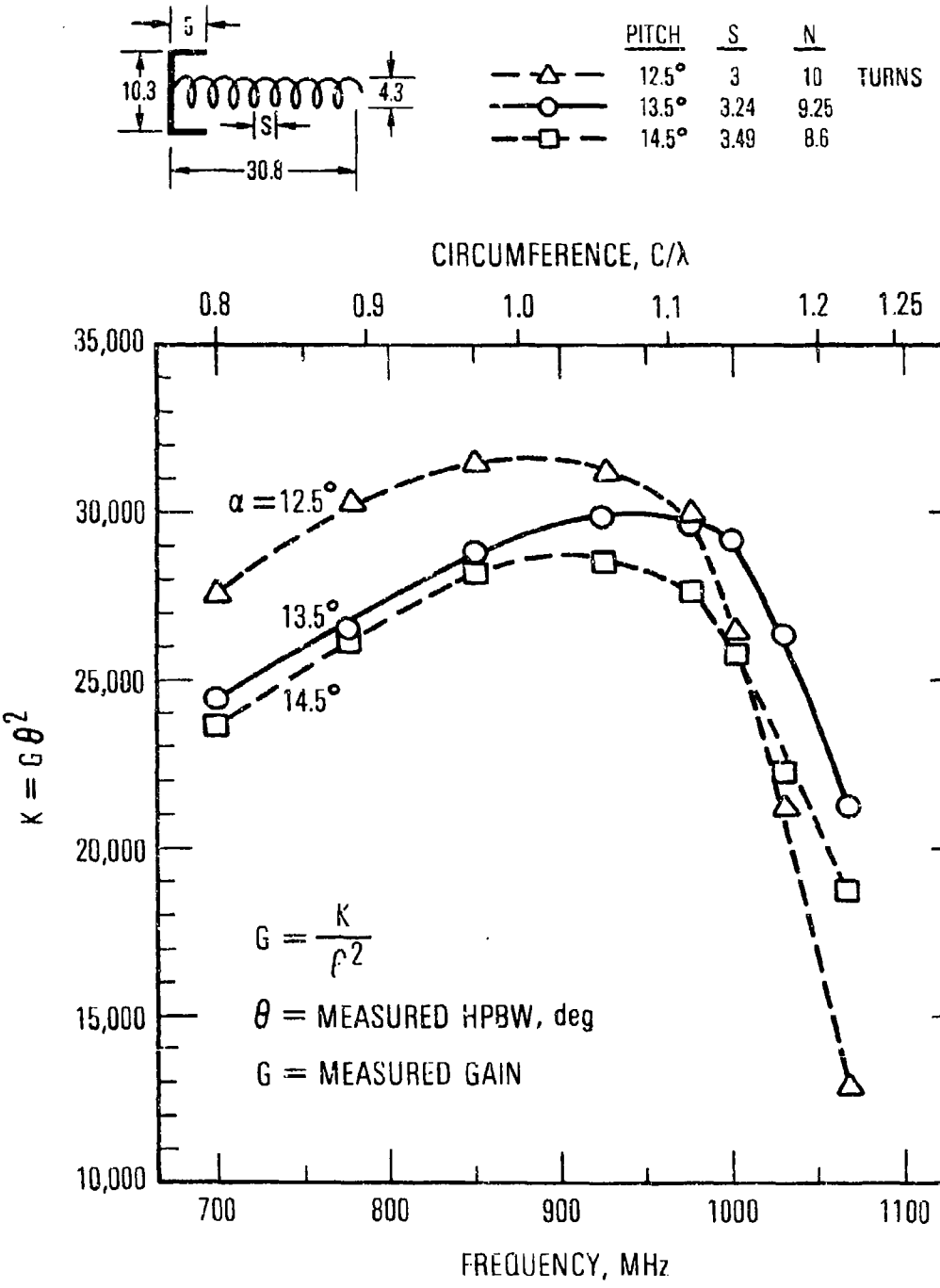

Fig. 12 Gain-Beamwidth Product for Various Pitch Angles Based on the 30.8-in. Length, 4.3-in. Diameter Experimental Helix

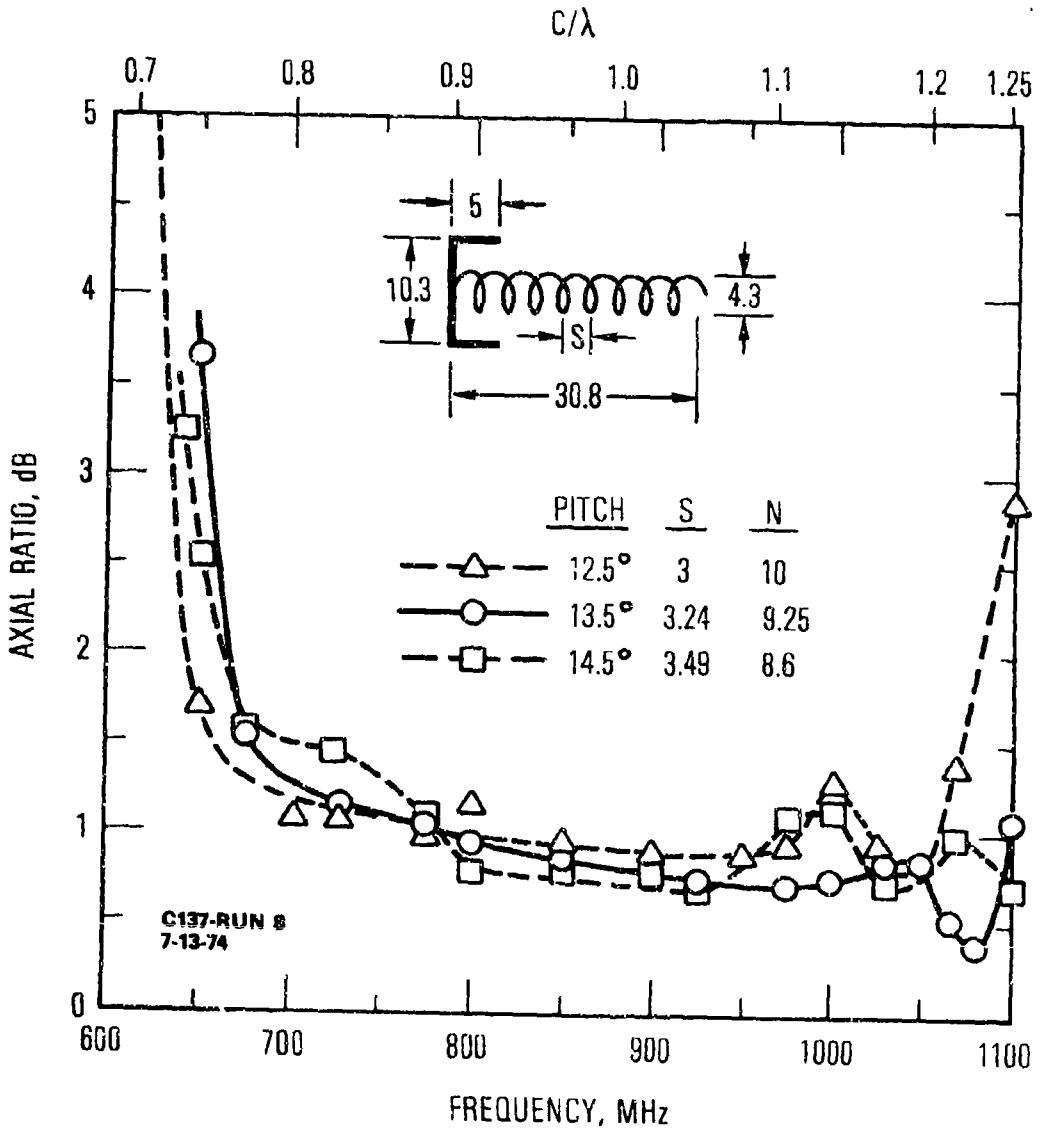

Fig. 13 Axial Ratios of a 30.8-in. Length and 4.3-in. Diameter Helix for Pitch Angles = 12.5°, 13.5° and 14.5°

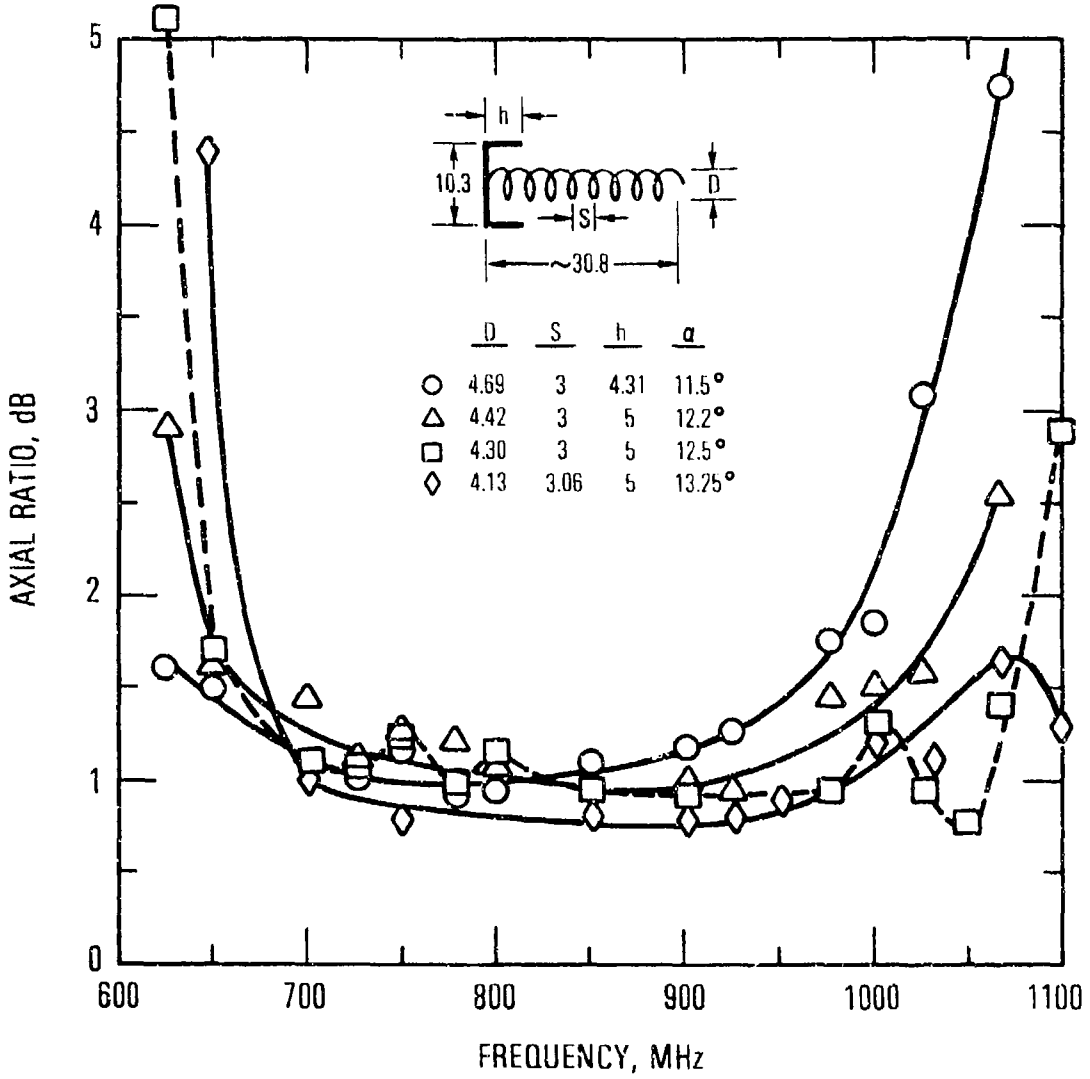

Fig. 14 Axial Ratios of a 10-turn Helix, 30.8-in. Long, for Diameters = 4.13 to 4.69 inches.

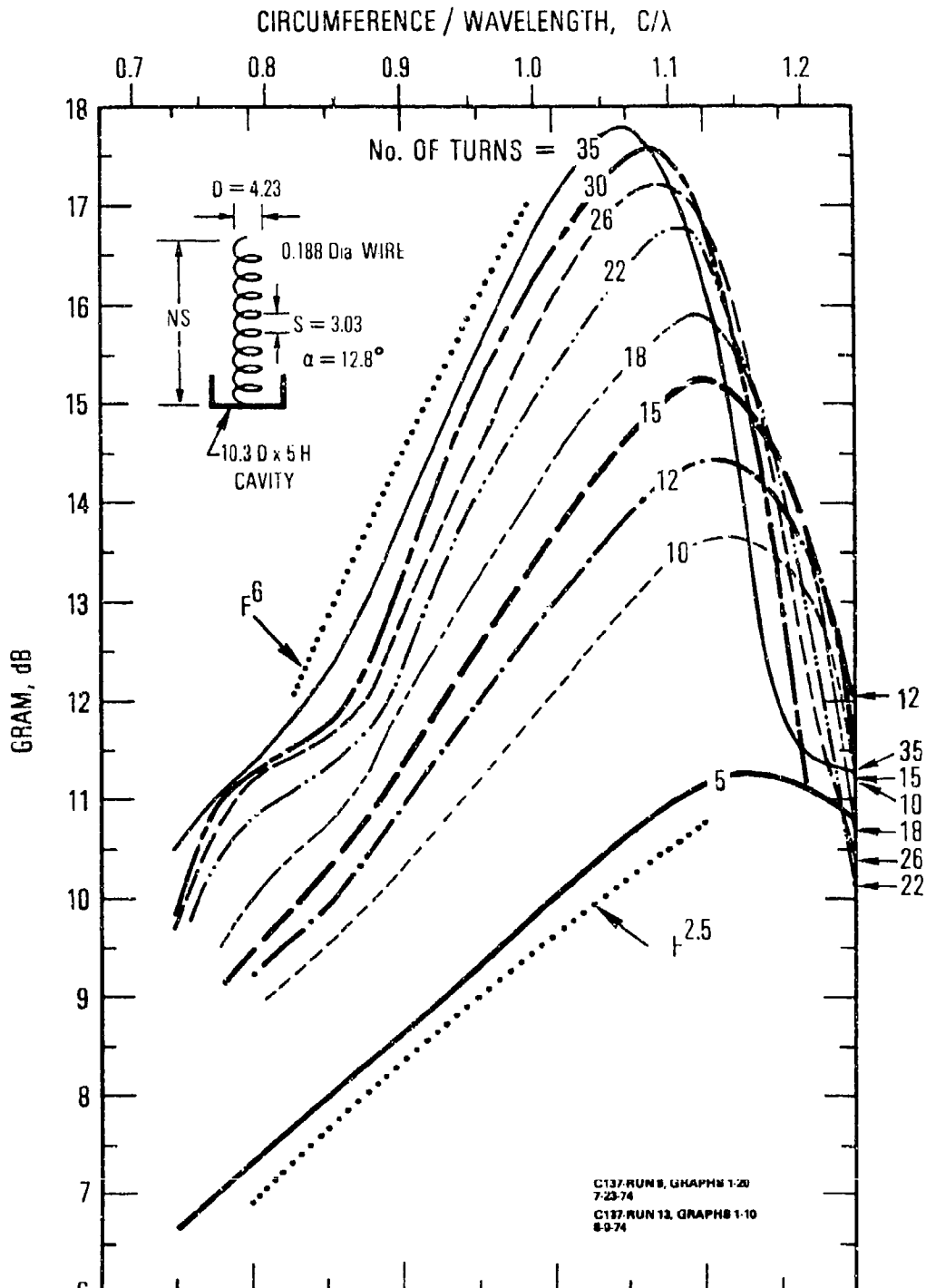

Fig. 15 Antenna Gain vs Frequency for the 5 to 35 Turn Helical Antennas, 4.23-in. Diameter

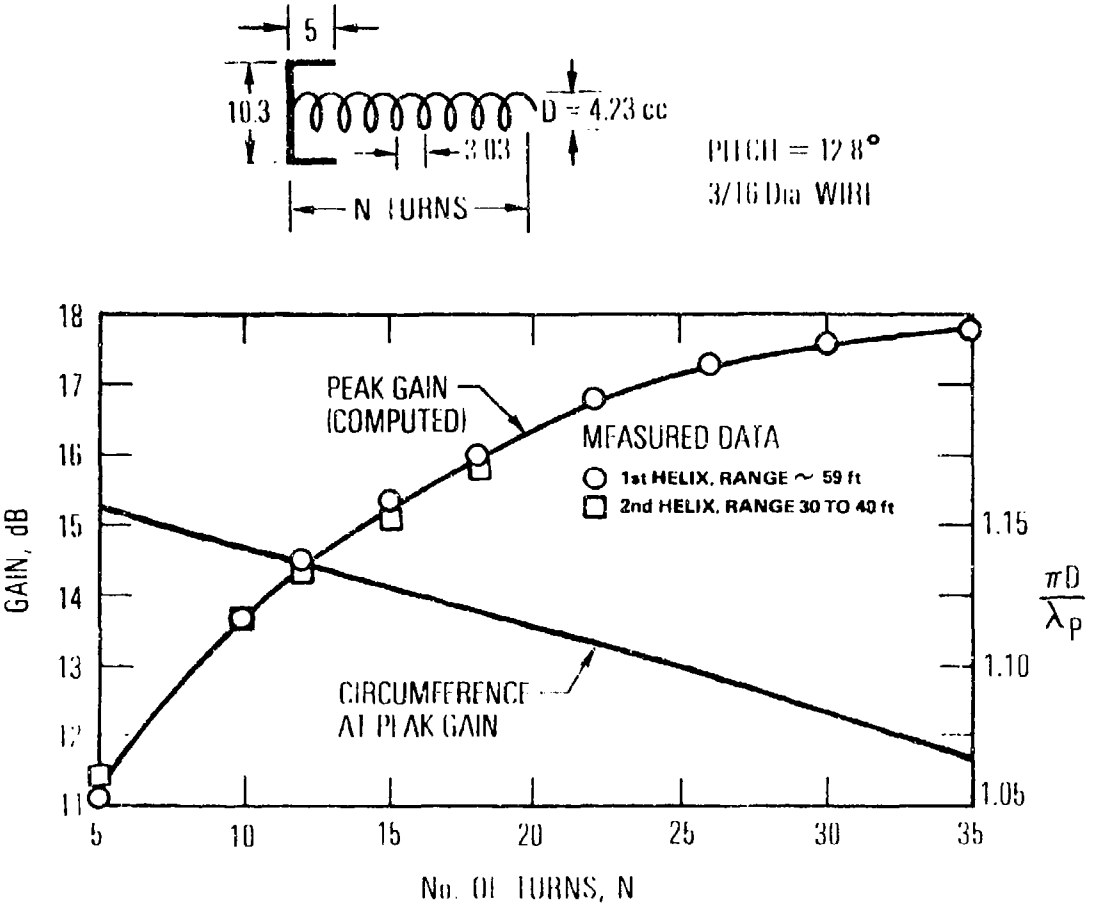

Fig. 16 Peak Gain Characteristics of a 4.23-in. Diameter 5 to 35 Turn Helix

in the figure, where λ_p is the wavelength at peak gain. The peak gain is not quite proportional to the number of turns; i.e., doubling the number of turns does not yield a 3 dB increase in the peak gain. An examination of the measured data shows that the gain varies approximately as $f^{\sqrt{N}}$ for $f < f_p/1.04$ and as $f^{-3\sqrt{N}}$ for $f > 1.03\, f_p$, where f_p is the frequency at peak gain. Based on this observation, the gain may be conveniently expressed as

$$G = \begin{cases} 0.91\, G_p \left(\dfrac{1.04}{f_p}\, f\right)^{\sqrt{N}} & ; \quad f \le \dfrac{f_p}{1.04} \\ G_p \quad ; \quad f = f_p & \\ 0.91\, G_p \left(\dfrac{f}{1.03\, f_p}\right)^{-3\sqrt{N}} & ; \quad f \ge 1.03\, f_p \end{cases} \tag{5}$$

where G_p is the peak gain from Eq. (1),

$$G_p = 8.3 \left(\frac{\pi D}{\lambda_p}\right)^{\sqrt{N+2}\,-1} \left(\frac{NS}{\lambda_p}\right)^{0.8} \left[\frac{\tan 12.5^\circ}{\tan 12.8^\circ}\right]^{\sqrt{N}/2} \tag{6}$$

Near the peak gain frequency, the gain may be approximated by a suitable mathematical function which has continuous derivatives and matches the gain at $f_p/1.04$, f_p, and $1.03\, f_p$. Equation (5) is accurate within $\pm$ 0.5 dB to the -5 dB points from the gain peak. The deviation is slightly larger for the shorter helices probably because the cavity influence is greater. Note that the pitch angle dependence was derived from the measured gain data on the 8.6- to 10-turn, constant length helices, and it is also valid for the present case, $\alpha = 12.8^\circ$ and N = 5 to 35 turns. The computed values for the peak gain are compared with the measured data in Fig. 16. The deviation is within $\pm$ 0.1 dB.

The gain-frequency response or bandwidth is of interest in practice. For the purpose of this study, we analyze the bandwidth by defining an allowable gain drop with respect to the peak gain, which in turn determines the frequency range. Figure 17 depicts the 3 dB and 2 dB bandwidths as a function of N. The choice between a 3 dB or 2 dB bandwidth would depend upon the particular application in question. If we denote the upper and lower frequencies by f_h and f_ℓ, respectively, then the bandwidth in percent may be expressed as

$$B = \frac{f_h - f_\ell}{\left(\frac{f_h + f_\ell}{2}\right)} \times 100\% \tag{7}$$

Using the empirical relations in Eq. (5), the bandwidth frequency ratio is approximately given by

$$\frac{f_h}{f_\ell} \approx 1.07 \left(\frac{0.91}{G/G_p}\right)^{4/(3\sqrt{N})} \tag{8}$$

The computed bandwidth characteristics for G/G_p = -3 dB and -2 dB agree reasonably well with the measured data as shown in Fig. 17. The bandwidth decreases as the axial length of the helix increases. This bandwidth behavior follows the same trends as described by Maclean and Kouyoumjian [Ref. 4], although these authors employ a sidelobe criterion rather than a gain criterion. Beyond the -3 dB point (with respect to the peak), the gain drops off sharply at the high-frequency end as the upper limit for the axial mode is approached.

The measured radiation patterns are shown in Figs. 18 to 26. The axial ratio is ~ 1 dB over most of the measurement frequency range and is slightly higher at the band edges. The patterns in the orthogonal planes are very similar and the HPBWs are within $\pm 1^\circ$. The HPBWs derived from these series of patterns are plotted in Fig. 27 with N as a parameter. At

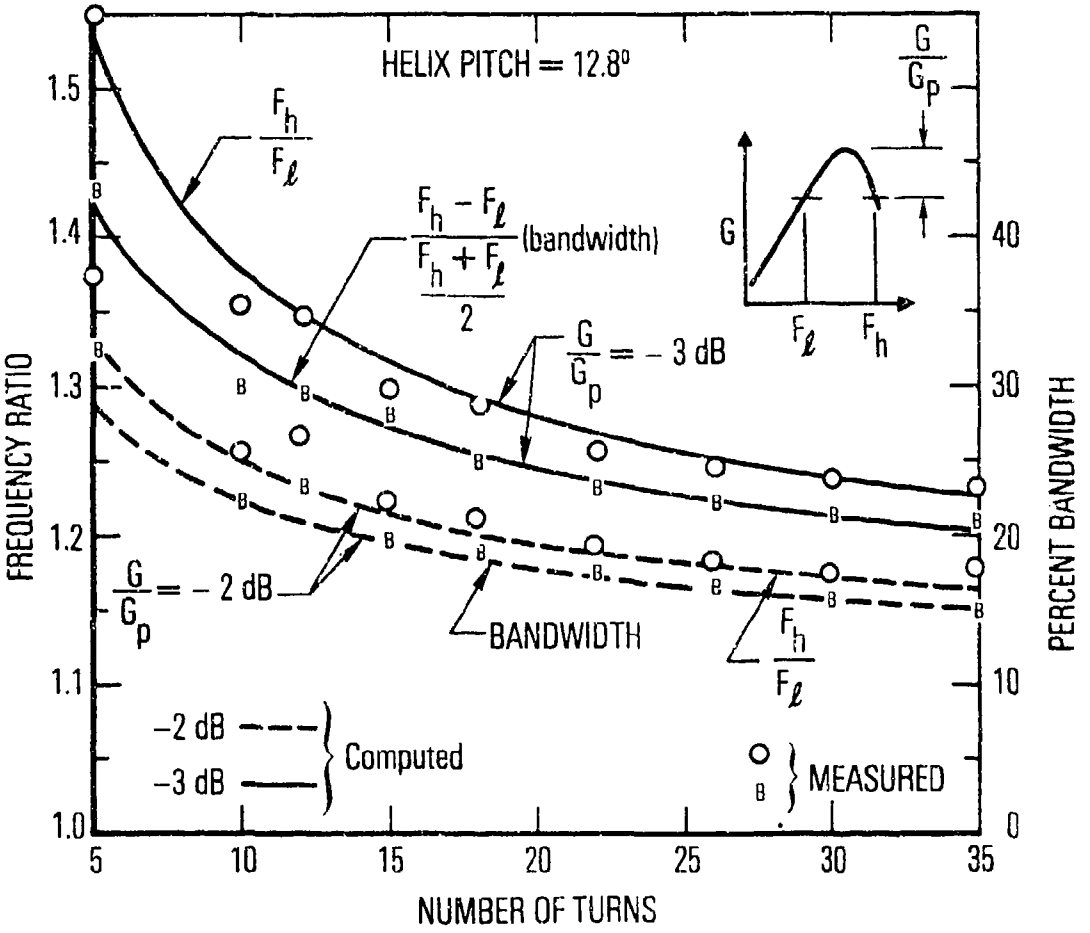

Fig. 17 Bandwidth Characteristics of a 4.23-in. Diameter 5 to 35 Turn Helix

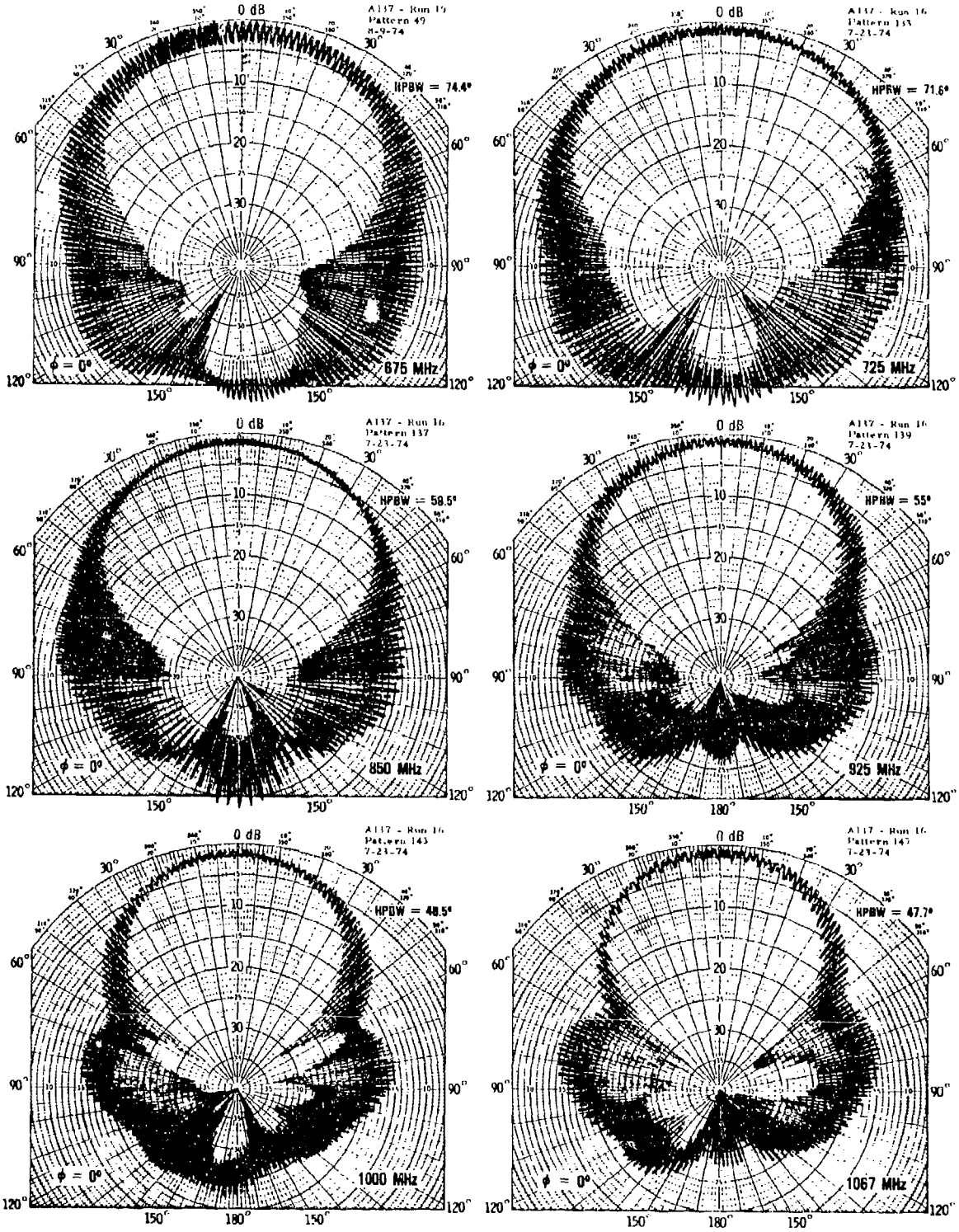

Fig. 18 Radiation Patterns of a 5-turn Helix — 4.23-in. Diameter and 12.8° Pitch Angle (S = 3.03 in.)

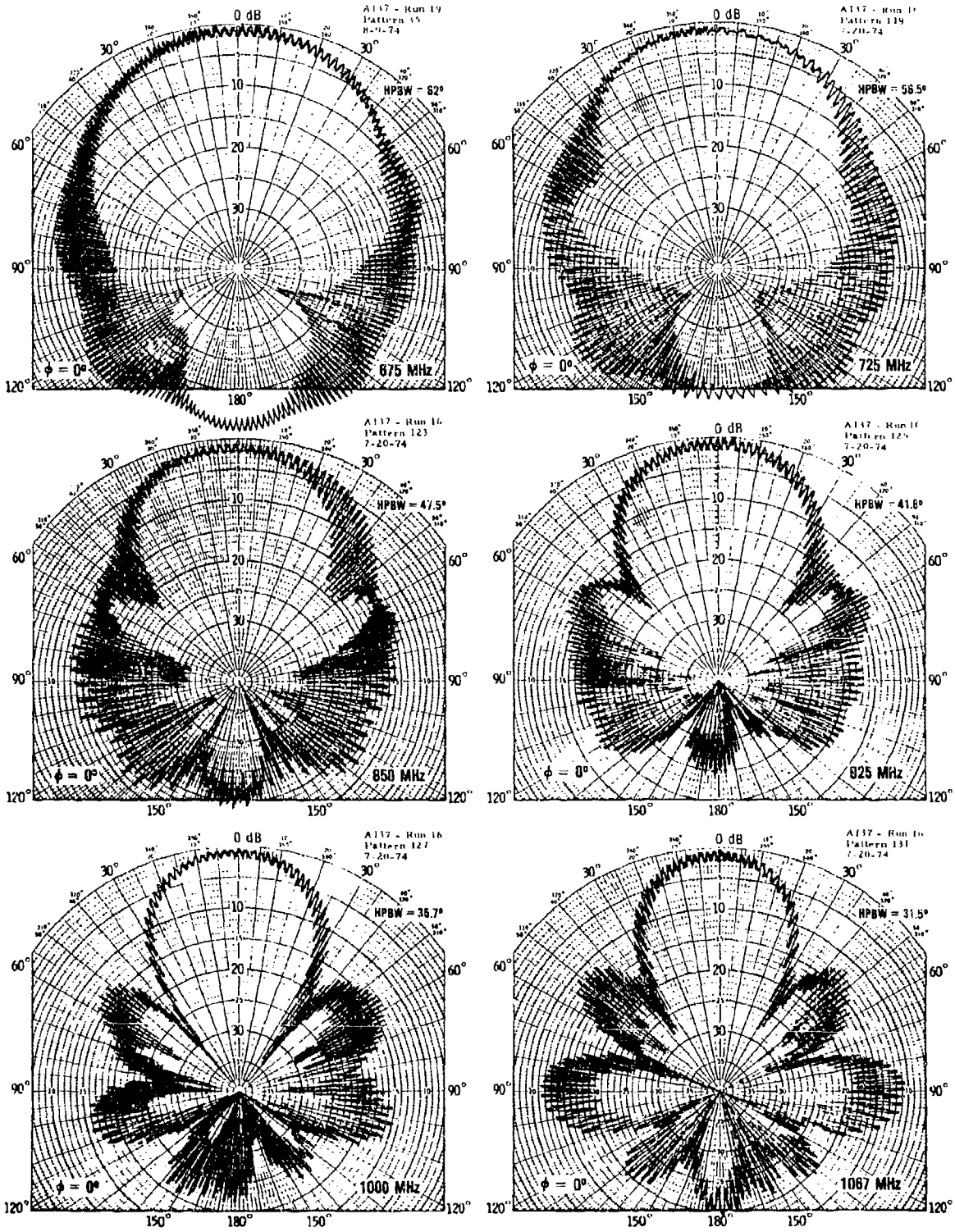

Fig. 19 Radiation Patterns of a 10-turn Helix — 4.23-in. Diameter and 12.8° Pitch Angle (S = 3.03 in.)

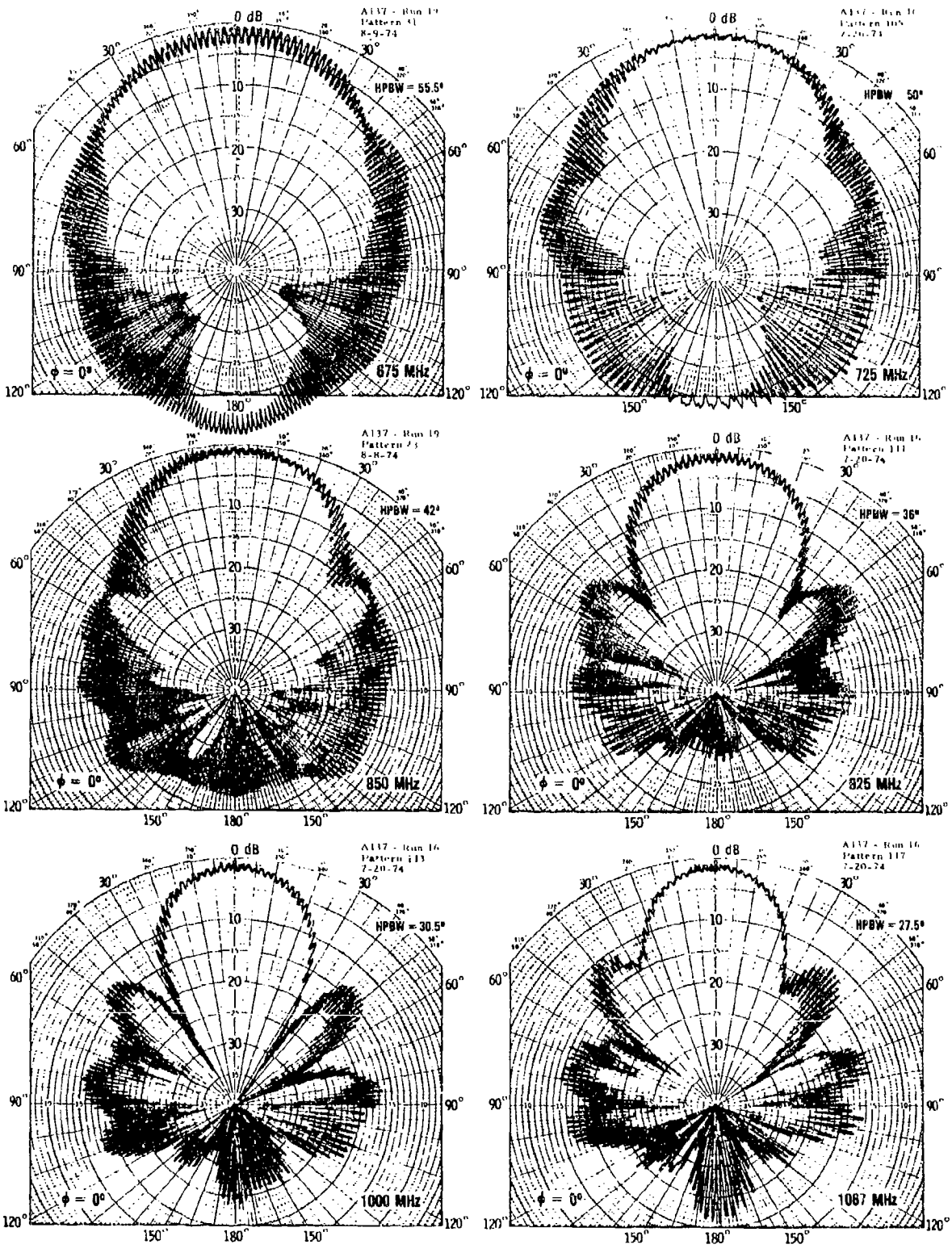

Fig. 20 Radiation Patterns of a 12-turn Helix — 4.23-in. Diameter and 12.8° Pitch Angle (S = 3.03 in.)

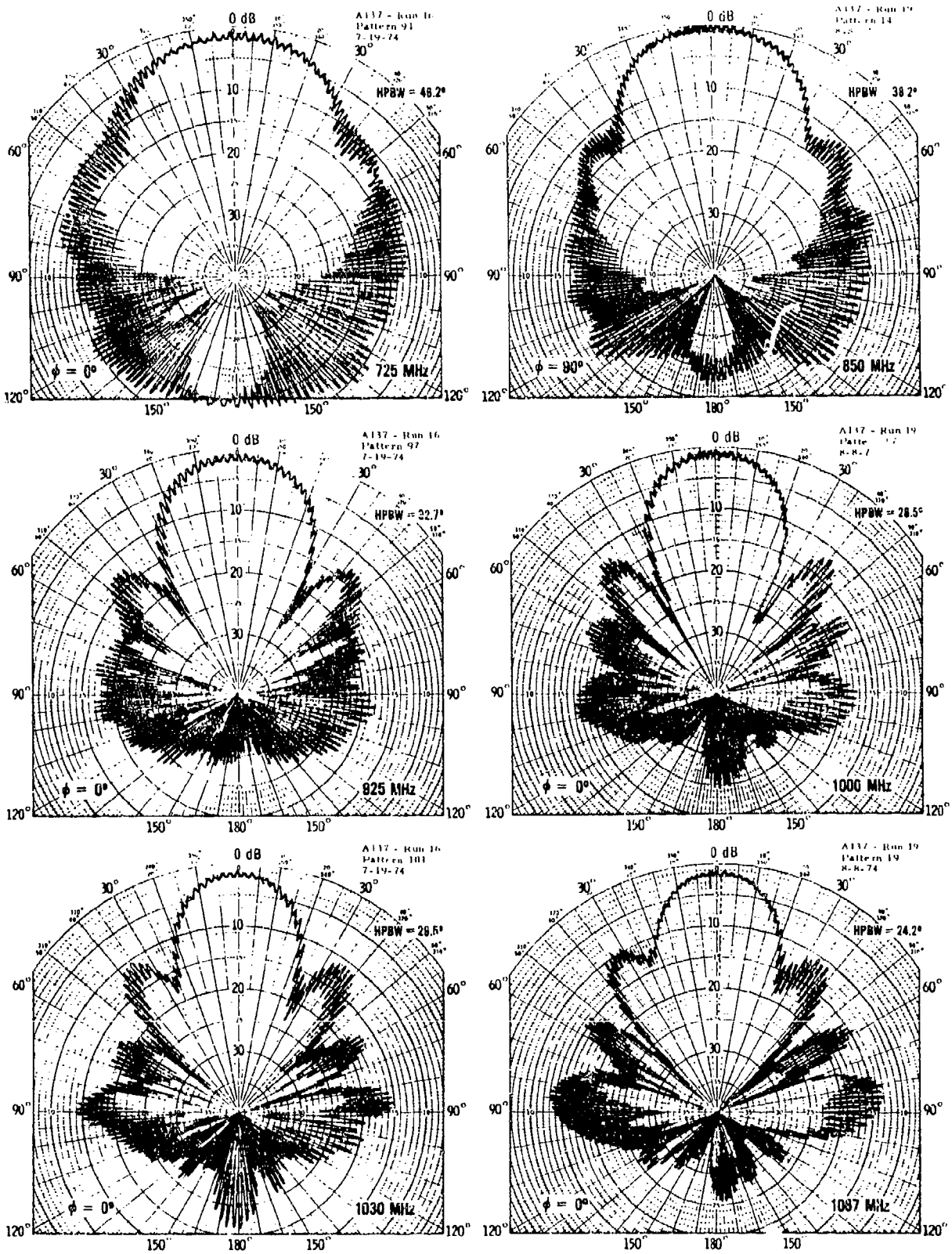

Fig. 21 Radiation Patterns of a 15-turn Helix — 4.23-in. Diameter and 12.8° Pitch Angle (S = 3.03 in.)

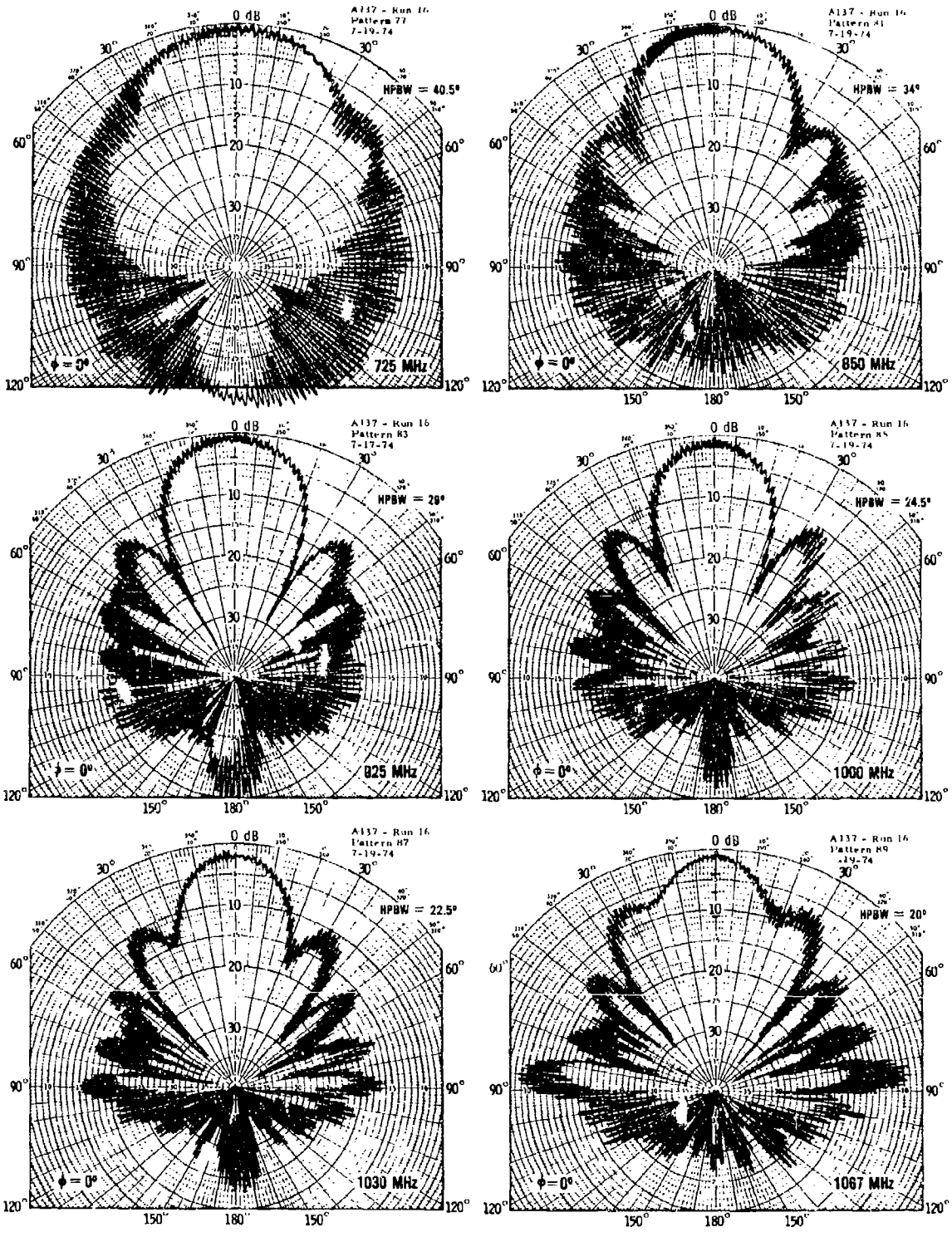

Fig. 22 Radiation Patterns of a 18-turn Helix — 4.23-in. Diameter and 12.8° Pitch Angle (S = 3.03 in.)

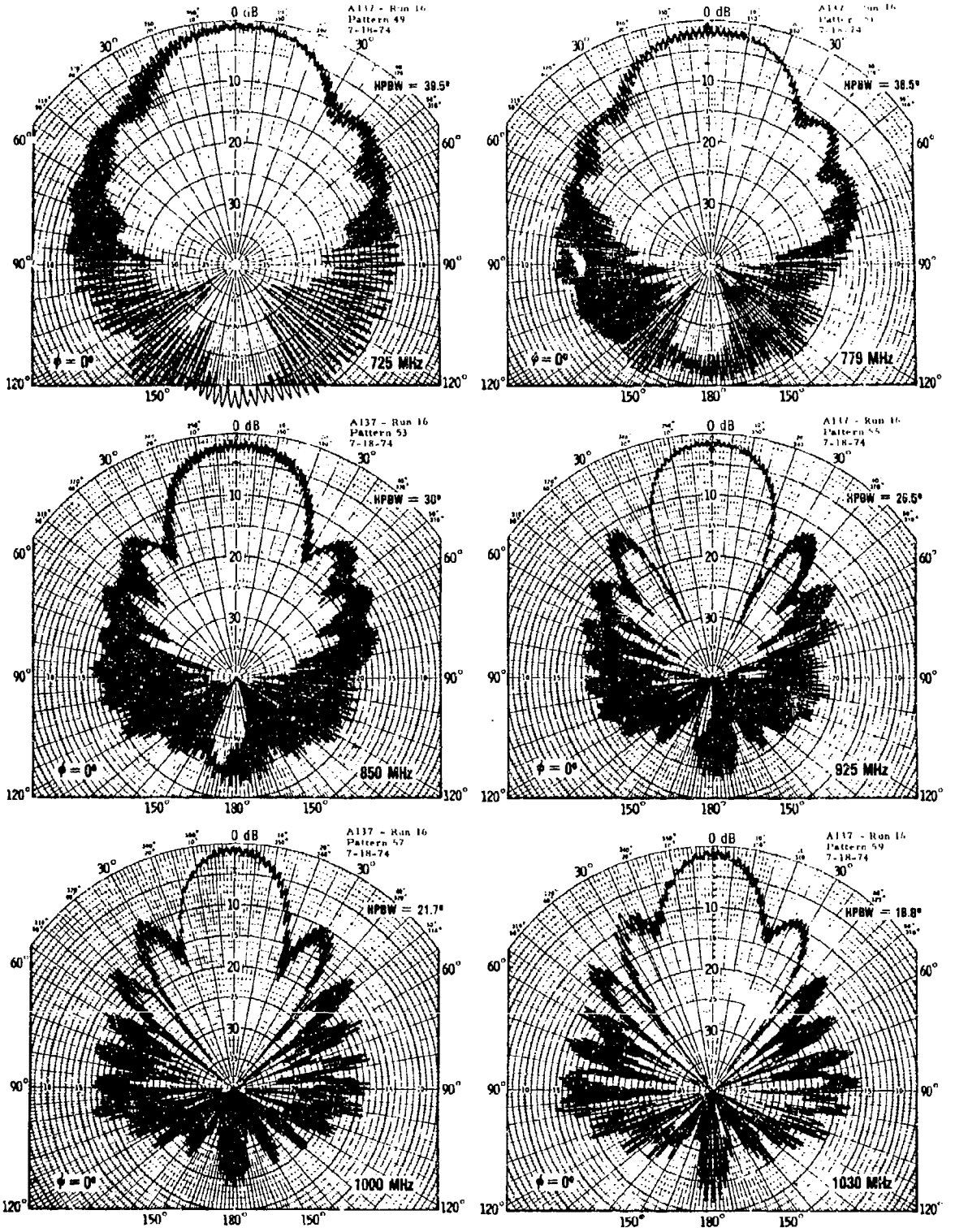

Fig. 23 Radiation Patterns of a 22-turn Helix — 4.23-in. Diameter and 12.8° Pitch Angle (S = 3.03 in.)

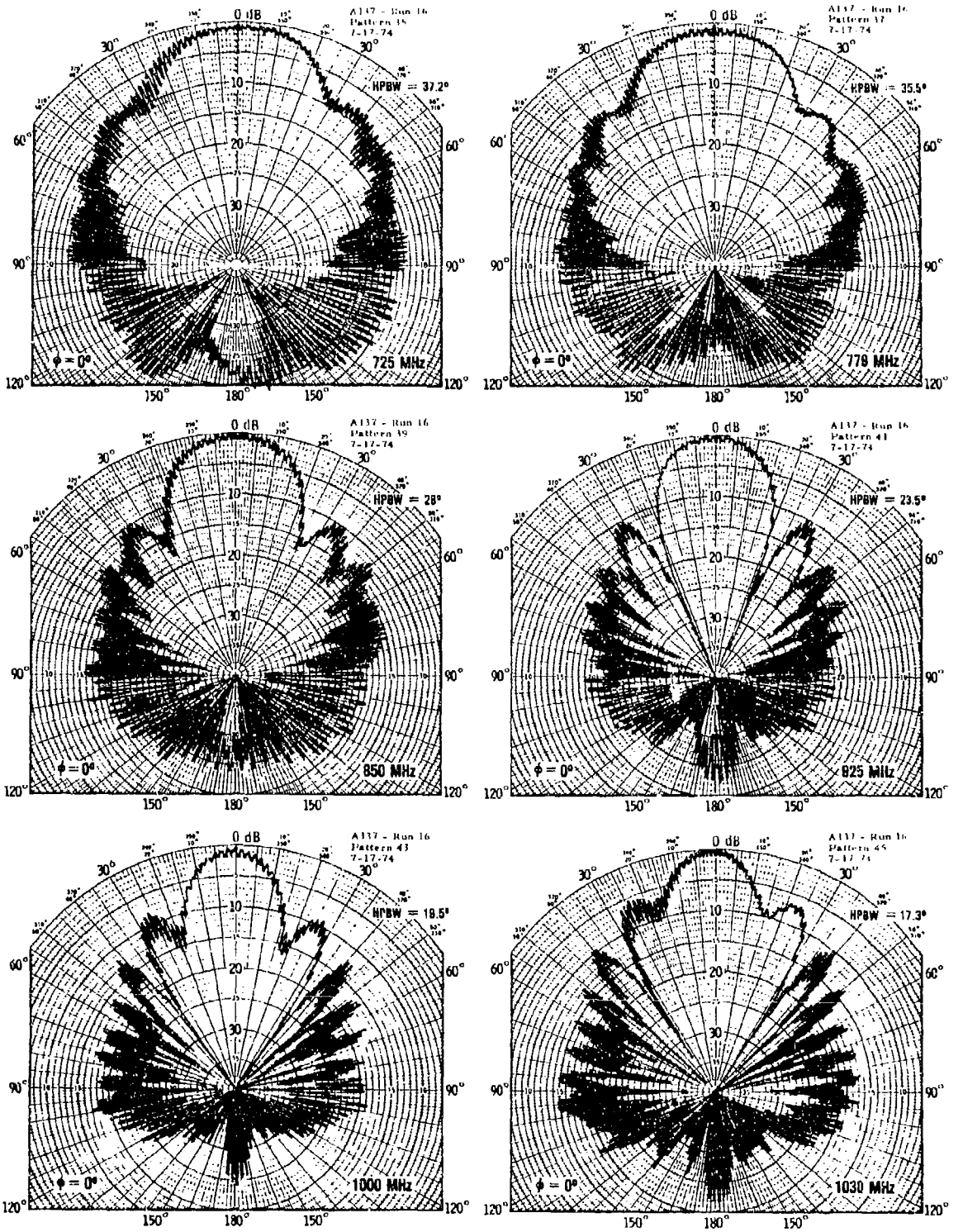

Fig. 24 Radiation Patterns of a 26-turn Helix — 4.23-in. Diameter and 12.8° Pitch Angle (S = 3.03 in.)

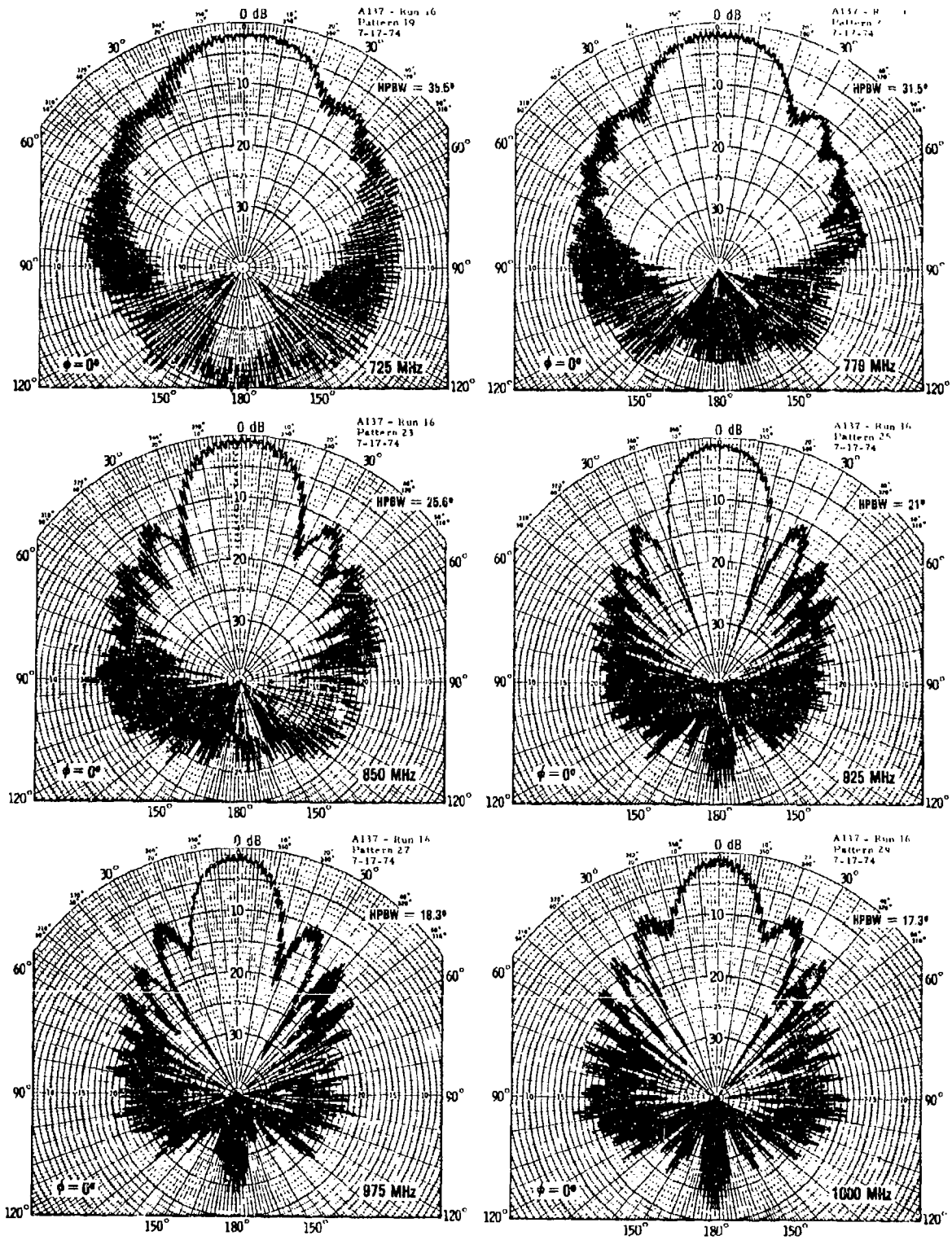

Fig. 25 Radiation Patterns of a 30-turn Helix — 4.23-in. Diameter and 12.8° Pitch Angle (S = 3.03 in.)

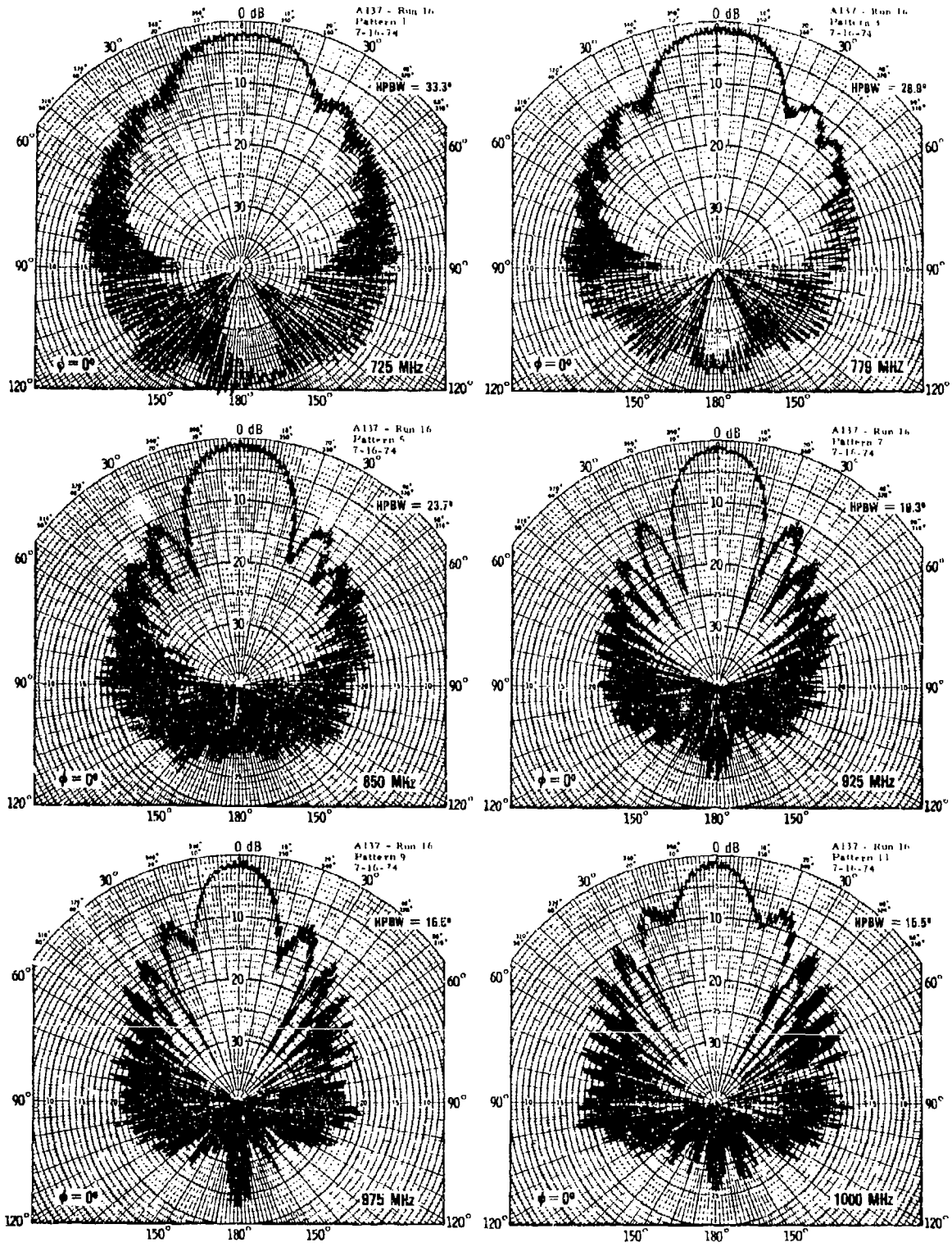

Fig. 26 Radiation Patterns of a 35-turn Helix — 4.23-in. Diameter and 12.8° Pitch Angle (S = 3.03 in.)

frequencies a few percent above the peak gain frequency, the patterns begin to deteriorate. The beamwidth broadens rapidly, and the first sidelobes merge in with the main lobe as the operating frequency approaches the upper limit. For the longer helices ($N > 22$), the beam broadening is particularly noticeable for $C/\lambda > 1.15$ as shown in Fig. 27.

Based on the gain data measured on the 4.23-in. diameter, constant pitch helices with $\alpha = 12.8^{\circ}$ and $N = 5$ to 35, parametric helix characteristic curves were derived in terms of the axial length and circumference with respect to wavelength. Figure 28 shows the gain as a function of axial length NS/λ with $\pi D/\lambda$ as a parameter. Thus, for a specified length and diameter the helix gain can be estimated. Figure 29 is a similar plot, except that gain is plotted as a function of the circumference $\pi D/\lambda$ with the axial length NS/λ (or L/λ) as a parameter. A similar parametric plot for the HPBW is shown in Fig. 30.

Figure 31 depicts the gain-HPBW product $K = G\theta^2$ based on the measured gain data of Fig. 15 and the HPBW data of Fig. 27. This quantity is useful for estimating the gain when the HPBW is known, and vice versa. The gain-HPBW product is not constant but depends on N and frequency. All curves have been smoothed to within $\pm$ 5% of the data points.

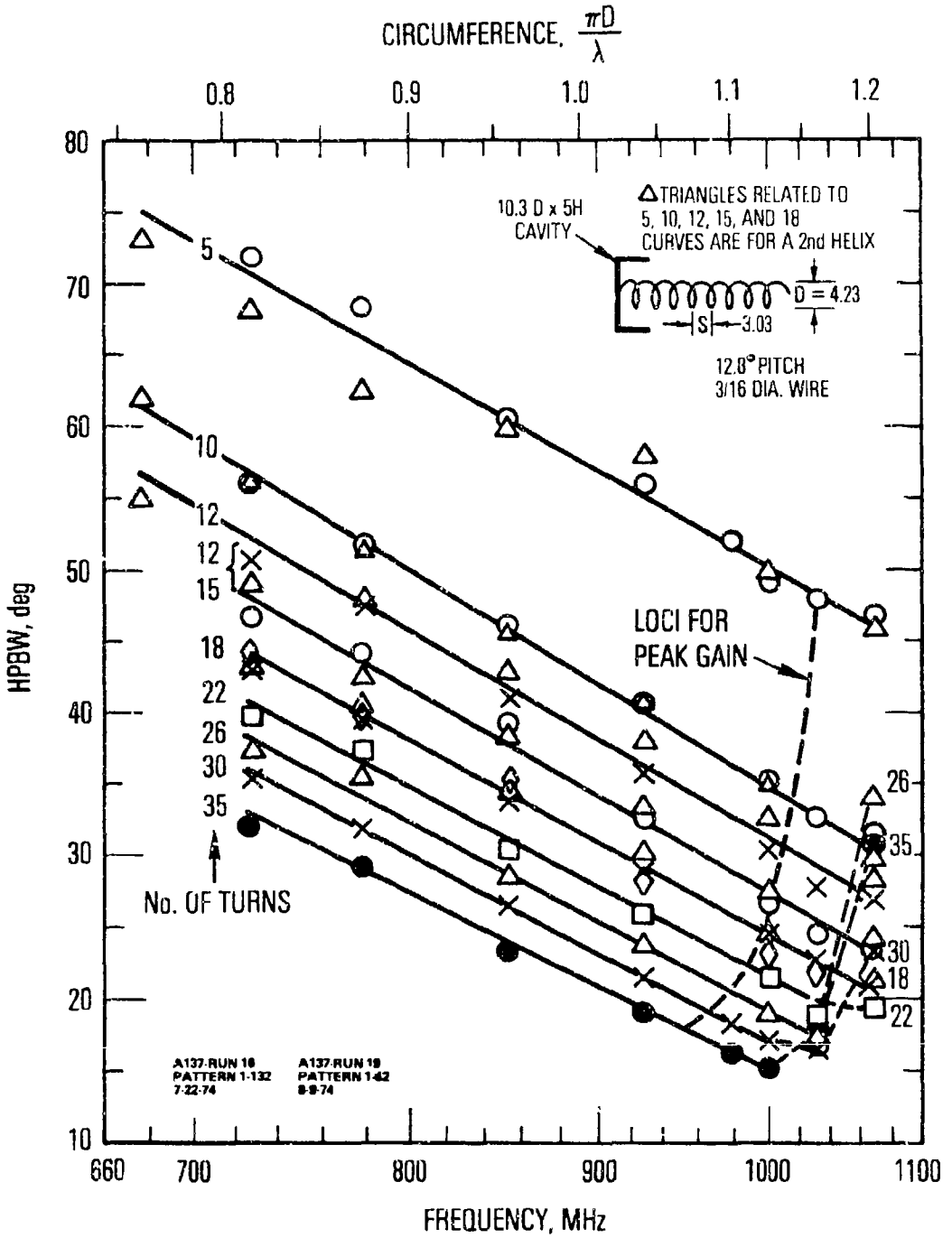

Fig. 27 Halfpower Beamwidths of 4.23-in. Diameter 5 to 35-turn Helix

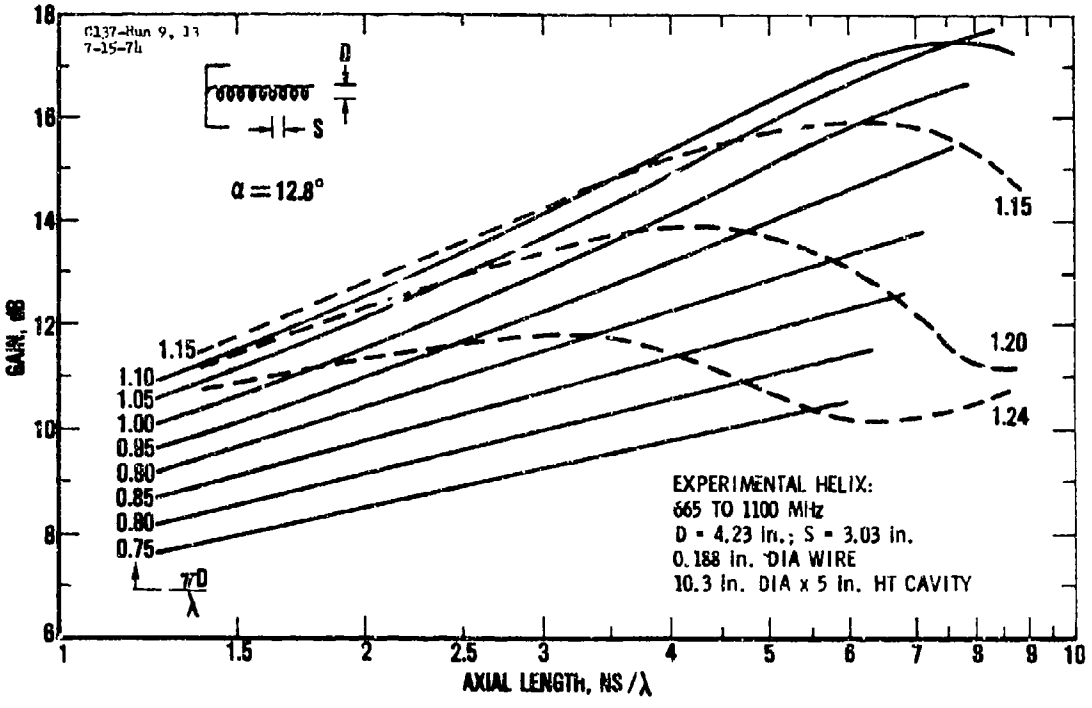

Fig. 28 Parametric Helix Antenna Gain Curves as a Function of Axial Length with Circumference as a Parameter

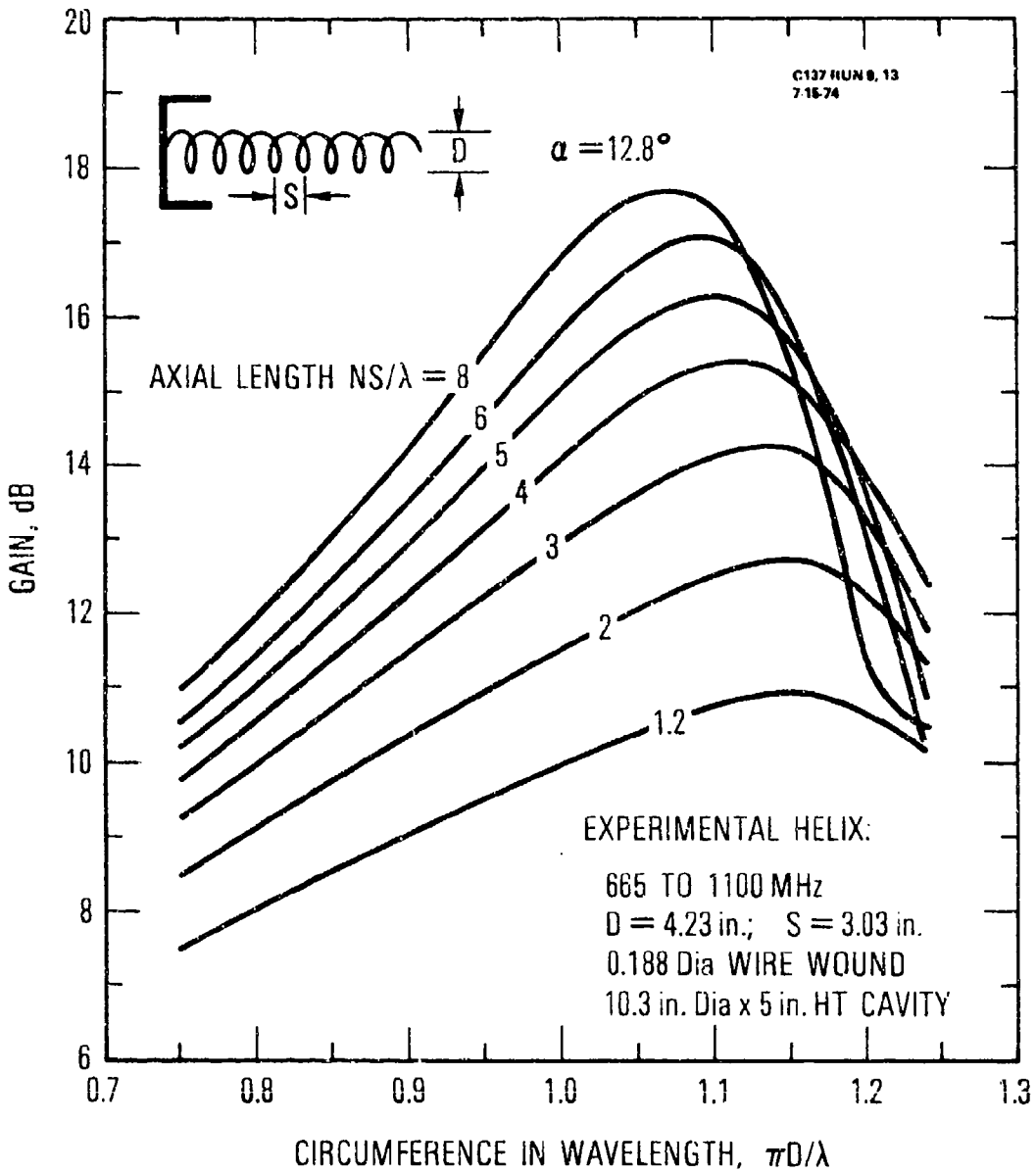

Fig. 29 Parametric Helix Antenna Gain Curves as a Function of Circumference C/λ with Axial Length L/λ as a Parameter

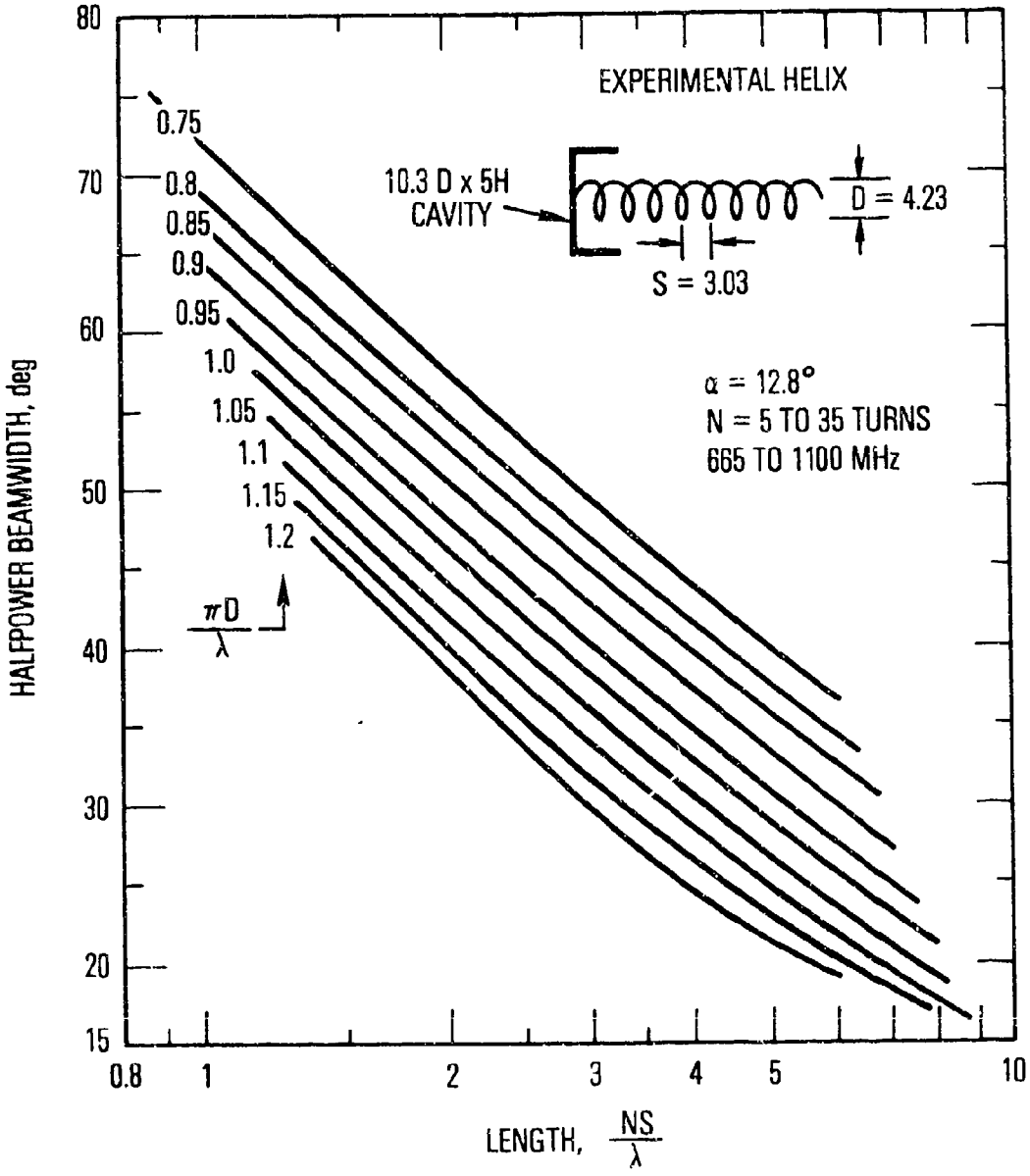

Fig 30 Helix Antenna Parametric Halfpower Beamwidth Curves as a Function of Axial Length with Circumference as a Parameter.

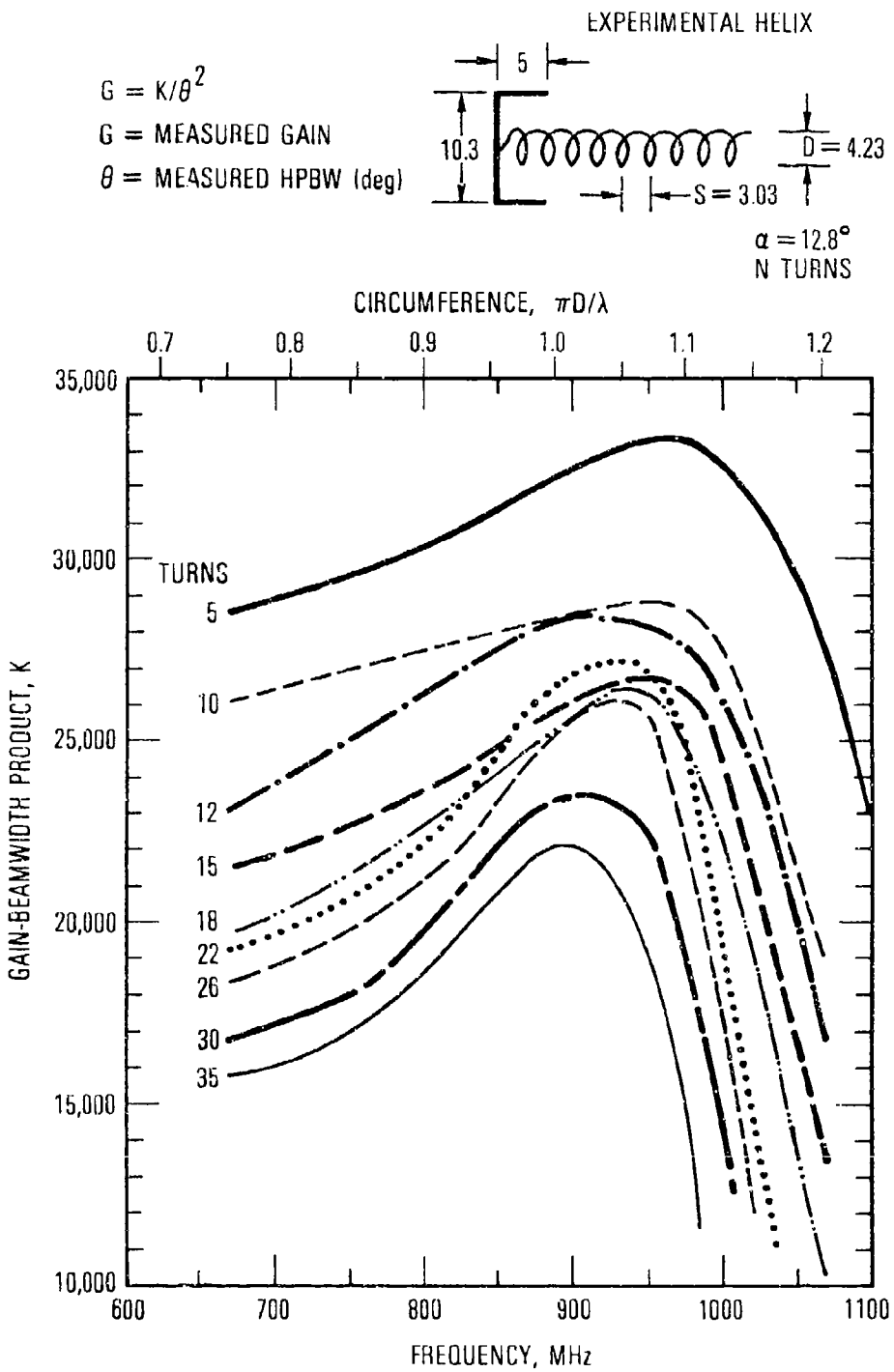

Fig. 31 Gain Beamwidth Products of the 5 to 35-turn Helical Antennas

IV. CONCLUSIONS

Based on a large amount of gain and pattern measurements, the performance characteristics have been established for a variety of helical antenna configurations. Parametric curves relating gain, HPBW, circumference C/λ and axial length NS/λ were derived and presented. Empirical expressions were derived for the antenna gain and bandwidth as a function of frequency and the helix design parameters. Generally, the peak gain occurs at a circumference C/λ that depends on the axial length, ranging from $C/\lambda \sim 1.07$ for a 35-turn helix to $C/\lambda \sim 1.15$ for a 5-turn helix. For $C/\lambda < 1$, the gain-frequency slope varies approximately as $f^{\sqrt{N}}$. At frequencies 5 to 10% above the peak gain frequency, the gain drops off sharply ($\propto f^{-3\sqrt{N}}$) and the pattern characteristics deteriorates rapidly as the helix upper frequency limit is approached. For a fixed diameter and length, a higher gain can be achieved with a smaller pitch angle, but a higher upper frequency limit is attained with a larger pitch angle. The bandwidth, when defined by the frequencies where the gain is 3 dB below the peak gain, narrows as the axial length increases, ranging from ~ 42% for $N = 5$ to 21% for $N = 35$.

The gain-beamwidth product, which is often of interest, is not constant and depends on the axial length and frequency. A larger value is attained with shorter length helices. On the average, the gain-beamwidth product varies from 18,000 for $N = 35$ and $0.75 < C/\lambda < 1.1$ to 31,000 for $N = 5$ and $0.75 < C/\lambda < 1.2$.

REFERENCES

1. J. D. Kraus, "Helical Beam Antenna," Electronics, 20, 109-111, (April 1947).

2. J. D. Kraus, Antennas, McGraw-Hill Book Co., New York (1950), Ch. 7.

3. E. F. Harris, "Helical Antennas," Ch. 7 of Antenna Engineering Handbook, Ed. by H. Jasik, McGraw-Hill Book Co., New York (1961).

4. T. S. M. Maclean and R. G. Kouyoumjian, "The Bandwidth of Helical Antennas," IRE Transactions on Antennas and Propagation, AP-7, Special Supplement, S379-S386, (December 1959).

5. T. S. M. Maclean and W. E. J. Farvis, "The Sheath-Helix Approach to the Helical Aerial," Proc. I.E.E., 109, Part C, 548-555, (1962).

6. T. S. M. Maclean, "An Engineering Study of the Helical Aerial," Proc. I.E.E., 110, 112-116, (January 1963).

7. K. G. Schroeder and K. H. Herring, "High-Efficiency Spacecraft Phased Arrays," AIAA 3rd Communications Satellite Systems Conference, Los Angeles, California April 6-8, 1970. AIAA Paper No. 70-425.

8. J. L. Wong and H. E. King, Broadband Quasi-Taper Helical Antennas, TR-0077(2724-01)-2, The Aerospace Corporation, El Segundo, Calif. (in publication).

9. D. J. Angelakos and D. Kajfez, "Modifications on the Axial-Mode Helical Antennas," Proc. IEEE, 55, 558-559 (April 1967).

10. S. Sander, D. K. Cheng, "Phase Center of Helical Beam Antennas," 1958 IRE National Convention Record, Pt. 1, 152-157 (March 1958).

11. R. J. Stegen, "The Gain-Beamwidth Product of an Antenna," IEEE Transactions on Antennas and Propagation, AP-12, 505-506 (July 1964).